Chemical Geology 470 (2017) 93–106

Contents lists available at ScienceDirect

Chemical Geology

journal homepage: www.elsevier.com/locate/chemgeo

Major transition of continental basalts in the Early Cretaceous: Implications for the destruction of the North China Craton

Kai Wu[a,f], Ming-Xing Ling[b,e,*], Weidong Sun[c,d,e,**], Jia Guo[a,f], Chan-Chan Zhang[a,f]

[a] CAS Key Laboratory of Mineralogy and Metallogeny, Guangzhou Institute of Geochemistry, Chinese Academy of Sciences, Guangzhou 510640, China
[b] State Key Laboratory of Isotope Geochemistry, Guangzhou Institute of Geochemistry, Chinese Academy of Sciences, Guangzhou 510640, China
[c] Center of Deep Sea Research, Institute of Oceanography, Chinese Academy of Sciences, Qingdao 266071, China
[d] Laboratory for Marine Mineral Resources, Qingdao National Laboratory for Marine Science and Technology, Qingdao 266237, China
[e] CAS Center for Excellence in Tibetan Plateau Earth Sciences, Chinese Academy of Sciences, Beijing 100101, China
[f] University of Chinese Academy of Sciences, Beijing 100049, China

ARTICLE INFO

Editor: K. Mezger

Keywords:
Ridge subduction
Alkali basalt
The Pacific plate
North China Craton
Lithosphere thinning

ABSTRACT

Geochemical compositions of continental basalts are generally considered as the best proxy record of the chemical and isotopic evolution of subcontinental lithosphere and convective mantle. There are voluminous Cretaceous continental basalts in the North China Craton (NCC), which are mainly composed of alkali basalts with minor sub-alkali basalts. Abrupt changes in chemical and isotopic compositions of these basalts were often ascribed to subcontinental lithosphere thinning of the NCC. However, processes responsible for such changes and its implications for subcontinental lithosphere evolution remain obscure. Here we report major geochemical changes at ~108 Ma in the north part of the NCC. The > 108 Ma alkali basalts are characterized by negative $\varepsilon_{Nd}(t)$ and declining "island arc-like" geochemical characteristics from the east to the west, implying decreasing slab-derived components from westward subducting slabs in their metasomatized lithospheric mantle sources. In contrast, the < 108 Ma Cretaceous alkali basalts have depleted Sr-Nd isotopic compositions and "OIB-like" geochemical features. These observations suggest that westward subduction of the Paleo-Pacific plate was responsible for the Cretaceous basaltic activities in the NCC. Combined with plate reconstructions and geophysical observations, we propose that flat subduction of the "extinct" ridge between the Izanagi and the Pacific plates controlled this major transition as well as the destruction of the NCC. The transition from a supra-subduction zone environment to a within-plate extensional environment around 108 Ma is probably due to the eastward slab rollback and the northward shift of the spreading ridge.

1. Introduction

There is increasing evidence that the subcontinental lithospheric mantle is dynamic, as indicated by changes in its thickness and containing components with varying geochemical and isotopic compositions through time (Farmer, 2014 and references therein). Continental basalts provide direct clues for the evolution of continental lithosphere and the underlying convective mantle. Previous studies recognized two types of continental basalts, namely basalts with similar geochemical compositions to ocean island basalts (OIB-like) and those resembling island arc basalts (Crow et al., 2010; Farmer, 2014; Fitton, 2007; Kempton et al., 2011). These two types of continental basalts, in some cases, erupted in the same region, e.g., the North China Craton (NCC) (Liu et al., 2008; Meng et al., 2015; Xu, 2001; Yang and Li, 2008). Origin and spatial-temporal changes of these basalts are crucial to decipher the evolution of continental lithosphere.

The NCC experienced the replacement of an ancient, thick and refractory lithospheric mantle by a young and fertile one through lithosphere thinning during the Mesozoic (Fan et al., 2000; Gao et al., 2008; Griffin et al., 1998; Ma et al., 2016; Menzies et al., 2007; Xu, 2001, 2014; H.F. Zhang et al., 2003), and the peak period of lithosphere thinning occurred at 130–110 Ma (Meng et al., 2015; Xu et al., 2004, 2009). Meanwhile, Cretaceous basalts in the NCC have also experienced a geochemical transition from "island arc-like" to "OIB-like" (Liu et al., 2008; Meng et al., 2015; Xu, 2001; Yang and Li, 2008; H.F. Zhang et al., 2003). It, however, still remains obscure that when and how such a transition happened beneath the NCC, and what implications for lithosphere evolution can be obtained. Liu et al. (2008) proposed a major

* Correspondence to: M.-X. Ling, State Key Laboratory of Isotope Geochemistry, Guangzhou Institute of Geochemistry, Chinese Academy of Sciences, Guangzhou 510640, China.
** Correspondence to: W. Sun, Center of Deep Sea Research, Institute of Oceanography, Chinese Academy of Sciences, Qingdao 266071, China.
E-mail addresses: mxling@gig.ac.cn (M.-X. Ling), weidongsun@gig.ac.cn (W. Sun).

http://dx.doi.org/10.1016/j.chemgeo.2017.08.025
Received 31 May 2017; Received in revised form 11 August 2017; Accepted 29 August 2017
Available online 04 September 2017

geochemical transition from “island arc-like” to “OIB-like” in the NCC at ~110 Ma. This study and subsequent researches by Yang et al. (2012) and Meng et al. (2015), however, comprised alkali basalts from Fangcheng (124.9 Ma), Feixian (119 Ma), Sihetun (125–124 Ma), Fuxin (107–94 Ma), Qujiatun (81.6 Ma) and Daxizhuang (73 Ma) and sub-alkali basalts from Yixian (125–122 Ma). No basalts erupted between 120 Ma and 107 Ma were discussed in these studies. The geochemical transition of Cretaceous basalts is ascribed to changes in their magma sources from the metasomatized lithospheric mantle to the asthenosphere (Meng et al., 2015; Ma et al., 2014; Xu, 2001). The occurrence of asthenosphere-dominated melts was generally considered as a mark of accomplishment of the lithosphere destruction, because decompression melting of asthenosphere beneath ancient cratons can only occur when the lithosphere is thin enough (Ma et al., 2016; Mckenzie and Bickle, 1988; Xu, 2014). Therefore, some studies proposed that this change indicated that the lithosphere thinning has completed at ~110 Ma through a “rapid” delamination process (e.g. Gao et al., 2004; Meng et al., 2015; Wu et al., 2002). Such a lithosphere delamination process was also adopted to explain the recently discovered small amounts of ~121 Ma lamprophyres with OIB-like geochemical characteristics in Shandong peninsula (Ma et al., 2014; Ma et al., 2016). It has been suggested that these lamprophyres were derived from the asthenosphere, indicating that the ancient lithospheric mantle would have already been replaced by a juvenile one at ~121 Ma in the eastern margin of the NCC (Dai et al., 2016; Ma et al., 2014, 2016). In contrast, this geochemical transition was considered as a part of a prolonged thermal erosion process, because the long-lasting continental lithosphere-derived magmatism (180–90 Ma) was replaced by asthenosphere-derived basaltic rocks in the Late Cretaceous (Menzies et al., 2007; Xu, 2001; Xu et al., 2004), and the enriched components observed in the Early Cretaceous basalts were essentially absent in the Tertiary basalts due to decratonization (Lu et al., 2006; Xu, 2014).

In addition, processes associated with the subduction of the Paleo-Pacific plate (Ling et al., 2013; Sun et al., 2007), e.g., “basal hydration weakening” to transform the lithosphere into convective asthenosphere (Guo et al., 2014; Niu, 2005; Niu et al., 2015), perturbing the hydrous mantle transition zone by the subducting Izanagi plate to release water for hydroweakening the lithospheric mantle (Kusky et al., 2007; Wang et al., 2016), slab rollback-induced unstable mantle flows (Sun, 2015; Wang et al., 2016; Zhang et al., 2014; Zhu et al., 2011, 2015; Zhu et al., 2012a, 2012b; Zhu and Zheng, 2009) or ridge subduction in the Early Cretaceous (Li et al., 2014; Ling et al., 2009, 2013; Sun et al., 2007), have also been proposed to explain the lithosphere destruction of the NCC. If subduction of the Pacific plate was the controlling factor, the question is what kind of signatures of plate subduction can be seen from those Cretaceous basalts?

Here we use a more complete geochemical dataset to explore spatial and temporal evolution of Cretaceous basalts in the NCC, as well as their relationship to the westward subduction of the Paleo-Pacific plate. Combined with plate reconstructions, geophysical observations and geological records of surrounding tectonic units, we also provide new insights into the petrogenesis of continental basalts, the evolution of the lithospheric mantle and the tectonics at the eastern Asian continental margin in the Cretaceous.

2. Geological background

The NCC is comprised of the east and the west blocks separated by the Proterozoic Trans-North China Orogen, which geographically corresponds to the Taihang Mountains (Guo et al., 2014; H.F. Zhang et al., 2003; Zhao et al., 2001). The Tan-Lu fault cut across the east part of the NCC (Xu, 2001) (Fig. 1). After collision between the east and the west blocks at ~1.8 Ga, the NCC remained stable until the Mesozoic (Gao et al., 2004; Griffin et al., 1998; Xu, 2001; Zhu et al., 2012a). Late Ordovician diamondiferous kimberlite reveals a cold, thick lithosphere of ~200 km (Fan and Menzies, 1992; Gao et al., 2002; Griffin et al., 1998; Menzies et al., 2007; Wu et al., 2006; Xu et al., 2004). However, studies on Late Cretaceous and Cenozoic basalts and mantle xenoliths indicate that the lithosphere has been thinned to ~60 km (Ma et al., 2016; Menzies et al., 2007; Wu et al., 2005; Xu, 2001, 2014; Zhang and Zheng, 2003). Therefore, > 100 km lithospheric mantle is inferred to have been removed during the Mesozoic (Fan and Menzies, 1992; Gao et al., 2008; Griffin et al., 1998; Wu et al., 2005; Xu, 2001; Zhu et al., 2012a).

Although the timing for lithosphere destruction of the NCC still remains controversial, it is generally accepted that the most intense period for lithospheric thinning was the Early Cretaceous, as suggested by occurrence of voluminous magmatic activities and significant mineralization (Gao et al., 2008; Menzies et al., 2007; Wu et al., 2005; Xu et al., 2004). Cretaceous basalts spread throughout the east block of the NCC. These basalts are mainly composed of alkali basalts with minor sub-alkali basalts (Fig. 1 and Table S1). Sub-alkali basalts are only outcropped in regions adjacent to the Tan-Lu Fault (Fig. 1). In contrast, alkali basalts are distributed even in the interior of the NCC (Fig. 1). Jining is the westernmost site that has > 108 Ma alkali basalts in the NCC reported so far, which is located at the western block of the NCC (Guo et al., 2014). In this contribution, a more complete dataset for Cretaceous basalts from the NCC including those formed between 120 and 107 Ma are used for the following discussion. Accurate intruding ages for these basalts are well constrained by various means, and all chemical data are from literatures without any artificial selection. More details about the geochronological and geochemical dataset are available in the “Supplementary materials”. Crustal assimilation for each basaltic intrusion is precluded in corresponding data source, which has also been summarized in the “Supplementary materials”. In addition, since experiments have shown that alkali basalts was produced at higher pressures than sub-alkali basalts (DePaolo and Daley, 2000; Falloon et al., 1988), variations in basalt compositions may partly result from vertical mantle heterogeneity. In order to minimize these disturbances, alkali and sub-alkali basalts are treated separately in the following sections.

3. Major transitions in Cretaceous basalts

Previous studies indicate that the isotopic and geochemical change of the Cretaceous basalts in the NCC occurred at the end of the Early Cretaceous (Liu et al., 2008; Meng et al., 2015; Xu, 2001; Yang and Li, 2008; Yang et al., 2012). The Cretaceous basalts in the NCC can be divided into two groups according to their Nd isotopic compositions: basalts formed before 108 Ma with negative $\varepsilon_{Nd}(t)$ and those formed after 108 Ma with positive $\varepsilon_{Nd}(t)$ (Fig. 2). Basalts formed before 108 Ma in the NCC exhibit enriched and generally variable Sr-Nd isotopic compositions. The Fangcheng basalts and the Feixian basalts have the lowest $\varepsilon_{Nd}(t)$ and the highest $(^{87}Sr/^{86}Sr)_i$ among these basalts. Chengde basalts and Xiaoling basalts show similar ε_{Nd} (t) with Fangcheng and Feixian basalts, but lower $(^{87}Sr/^{86}Sr)_i$. The rest of the > 108 Ma basalts have relatively high $\varepsilon_{Nd}(t)$ and moderate $(^{87}Sr/^{86}Sr)_i$, most of which lies within the field defined by Paleozoic kimberlite and peridotite. In contrast, the < 108 Ma Cretaceous basalts display depleted Sr-Nd isotopic composition, which are mostly plotted in the field defined by Cenozoic basalts in the NCC (Fig. 2).

The transition in geochemical compositions is illustrated in Fig. 3. The > 108 Ma alkali basalts are characterized by lower high field strength elements (HFSE), but generally higher and variable large ion lithophile elements (LILE) and LILE/HFSE, which overlaps the fields of arc magmas (Fig. 3). With the exception of the Jining basalts, all the > 108 Ma alkali basalts and all Cretaceous sub-alkali basalts have lower Nb contents (< 25 ppm). In contrast, the < 108 Ma Cretaceous alkali basalts have higher and variable HFSE (e.g. Nb > 25 ppm), but lower LILE concentrations and LILE/HFSE ratios. Interestingly, HFSE contents and Nb/Zr ratios of those < 108 Ma alkali basalts are positively correlated with Ba, Th, Pb/Zr and Ba/Zr (Fig. 3), which suggests

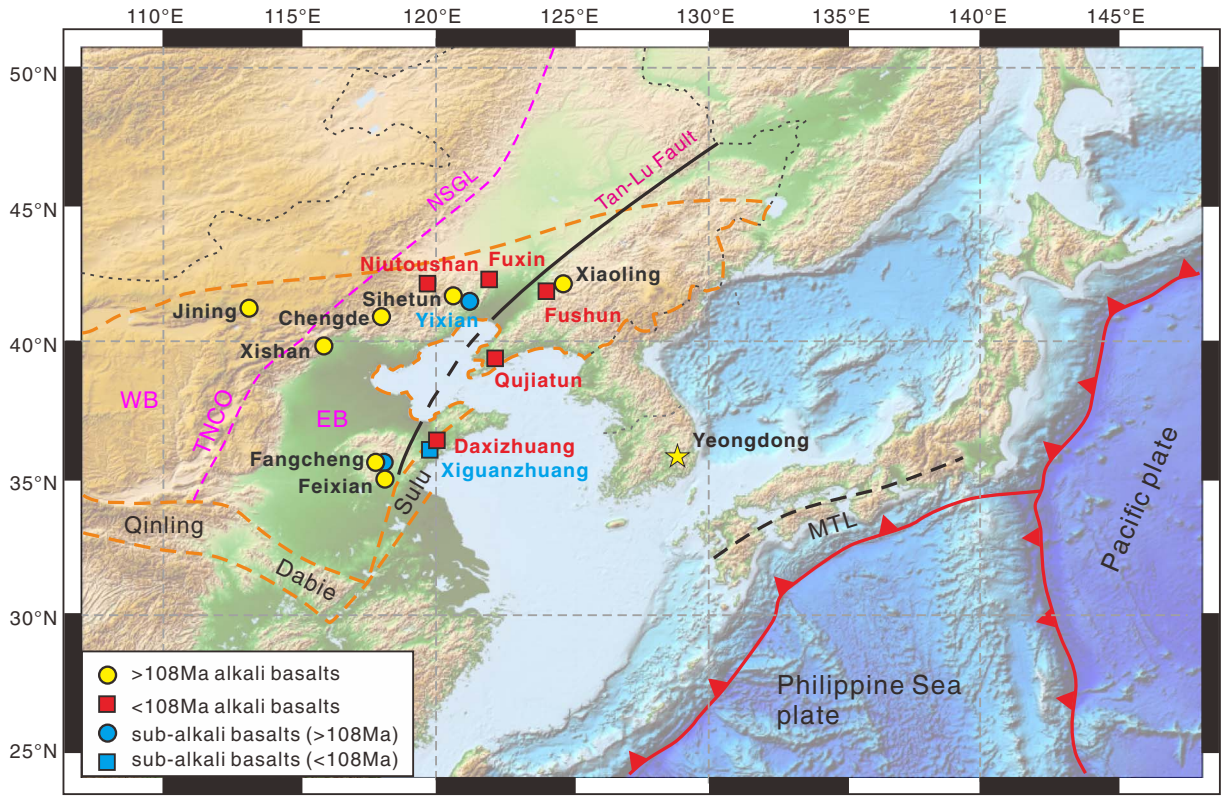

Fig. 1. Distributions of Cretaceous basalts in the North China (Sino-Korean) Craton. EB, TNCO and WB represent the east block, the Trans-North China Orogen and the west block, respectively. NSGL is the North-South Gravity Lineament. MTL denotes the Median Tectonic Line in Japan (Kinoshita, 1995). Cretaceous basalts from Yeongdong basin in South Korea (yellow star) are also shown for comparison. (For interpretation of the references to color in this figure legend, the reader is referred to the web version of this article.)

partial melting trends without major contributions from plate subduction.

The contrasting geochemical compositions can also be observed in the primitive mantle normalized spider diagram (Fig. 4), where the > 108 Ma basalts show positive Ba, Pb, Sr, La (LILE and LREE) anomalies and negative Nb, Ta, Zr, Hf (HFSE) anomalies, which is similar to arc basalts. However, the < 108 Ma Cretaceous basalts display similar distribution patterns with OIB, with only weak Ba, Pb and Sr positive anomalies (Fig. 4). In addition, the locations of these two types of alkali basalts in the NCC are also different. The > 108 Ma alkali basalts are distributed widely, even in the interior of the NCC, while the < 108 Ma Cretaceous alkali basalts appeared in restricted regions adjacent to the Tan-Lu Fault (Fig. 1).

Interestingly, the Jining basalts (119.6–108.6 Ma) are plotted near the fields defined by the < 108 Ma Cretaceous basalts in Fig. 3 and show similar trace element distribution patterns with these < 108 Ma basalts in Fig. 4. However, the negative ε_{Nd} (t) and higher $(^{87}Sr/^{86}Sr)_t$ make it quite different from the < 108 Ma Cretaceous basalts. Meanwhile, Jining basalts are also different from the > 108 Ma alkali basalts, because they have less enriched fluid mobile elements (e.g. Ba, Pb

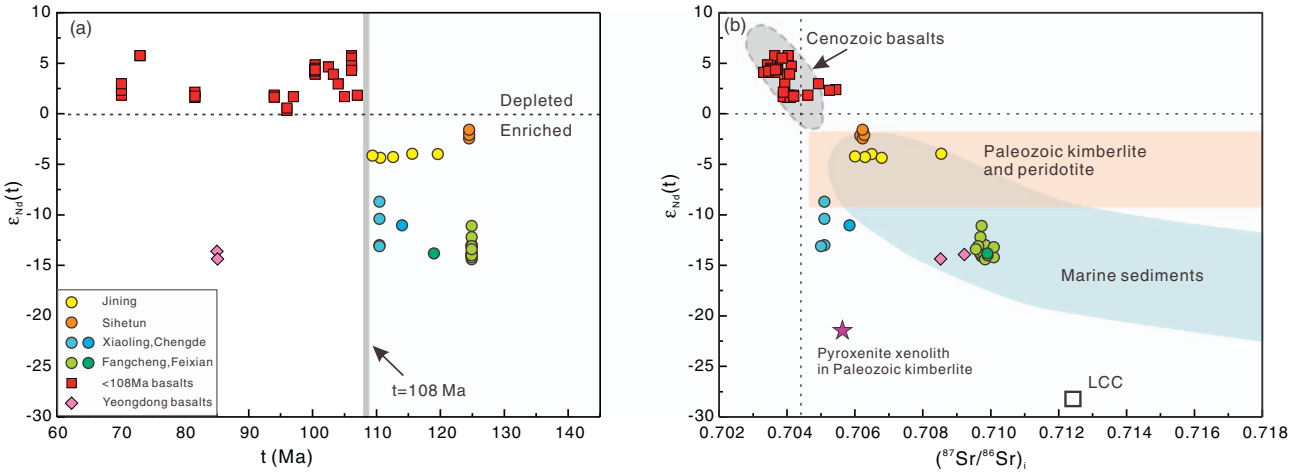

Fig. 2. Temporal variations in ε_{Nd}(t) and Sr-Nd isotopic composition of the Cretaceous basalts in the North China Craton. LCC represents lower continental crust of North China Craton, which is from Jahn et al. (1999). The Nd-Sr isotopic composition of lithospheric mantle beneath North China Craton is estimated from Paleozoic kimberlite and mantle xenoliths (Zheng and Lu, 1999; Zheng, 1999; H.F. Zhang et al., 2008; Yang et al., 2009). Isotopic compositions of pyroxenite xenoliths from the Mengyin kimberlites are from H.F. Zhang et al. (2008) and Y.Q. Zhang (2008). The Sr-Nd isotopic compositions for marine sediments are from Plank and Langmuir (1998).

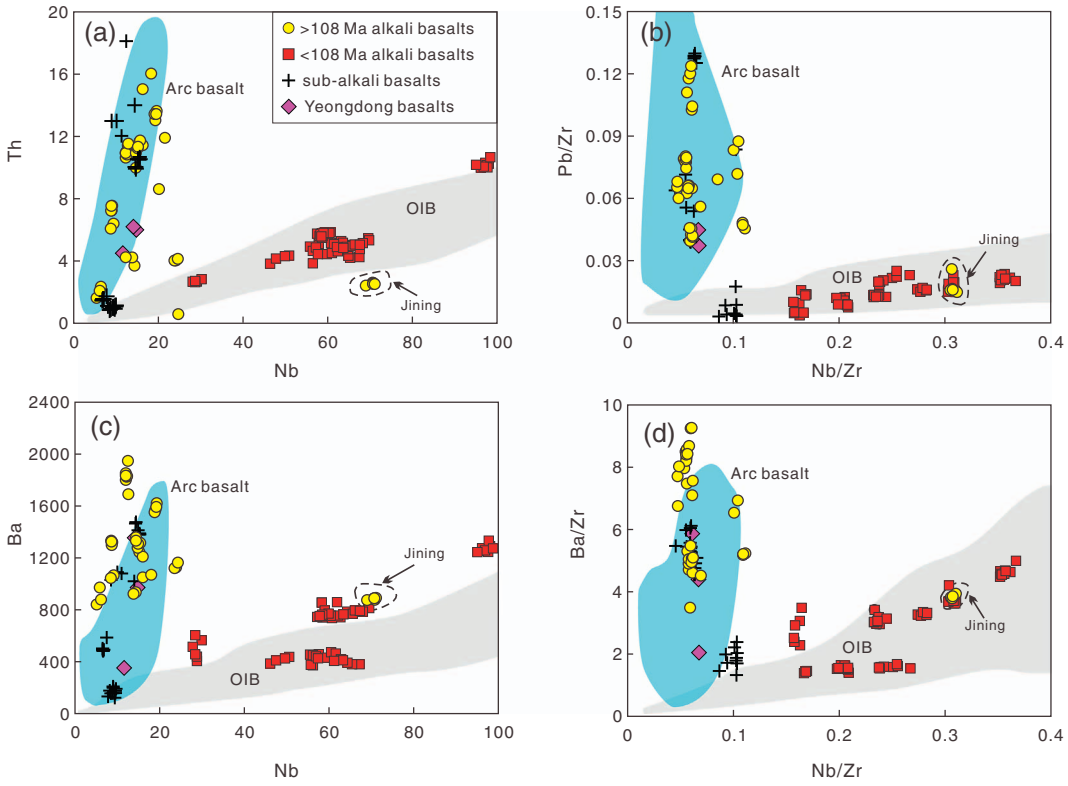

Fig. 3. Plots showing systematic divergent trends of the > 108 Ma and < 108 Ma alkali basalts in the NCC. Data for arc and OIB field are from Kelemen et al. (2003) and GEOROC: http://georoc.mpch-mainz.gwdg.de/georoc/.

and Sr) and no depletion of HFSE. Therefore, the Jining basalts were derived from the lithospheric mantle with insignificant enrichment of fluid mobile elements. In contrast, alkali basalts in Fuxin (107–94 Ma) display depleted Sr-Nd isotopic and OIB-like chemical compositions, whose primary source is asthenosphere. Then, a major transition in primary magma source of Cretaceous basalts in the NCC occurred at ~108 Ma, when the alkali basalts also changed from "arc-like" (the > 108 Ma alkali basalts) to "OIB-like" (the Niutoushan basalts: 107–94 Ma; the Fuxin basalts: 106.1 Ma).

4. Discussion

4.1. Fluid/melt metasomatism in mantle sources of the > 108 Ma alkali basalts

The enrichment of LILE and strong depletion of HFSE are generally taken as distinctive characteristics of arc magmas (Kelemen et al., 2003; Ormerod et al., 1988; Reiners et al., 2000) and the continental crust (Rudnick and Gao, 2003). The difference between the > 108 Ma and the < 108 Ma Cretaceous alkali basalts is mainly embodied in these elements (Fig. 4). The formation of arc magma is generally through flux melting of mantle wedge, where fluids/aqueous melts released by the subducted slab rise into the mantle wedge, lowering its solidus

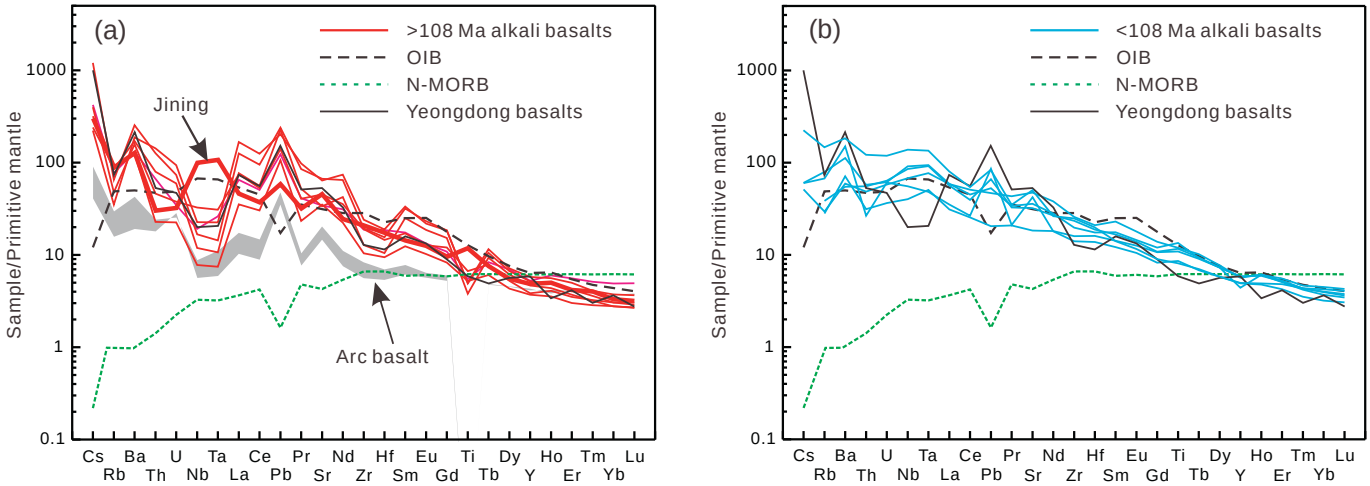

Fig. 4. Primitive mantle-normalized trace element diagrams for Cretaceous alkali basalts. Values for N-MORB, OIB and normalized data are from Sun and McDonough (1989). Field for arc basalt is from Kelemen et al. (2003).

temperature and triggering magma formation (Anderson, 1982; Gaetani and Grove, 1998; Johnson et al., 2009; McCulloch and Gamble, 1991). Partial melting of individual mantle sources metasomatized by varying proportions of subduction-released components has been shown to be responsible for trace element variations of arc magma suites (Reiners et al., 2000; Stolper and Newman, 1994). For example, arc magmas behind the volcanic front have lower H_2O and fluid mobile element contents, suggesting decreasing flux of H_2O-rich components from subducted slabs across the active subduction zone (Stolper and Newman, 1994; Walker et al., 2003). Regular across-arc decreasing fluid mobile element contents (e.g. B, As, Sb, Pb and Ba) and mobile/immobile element ratios of arc magma were thought to reflect progressive chemical depletion of the down-going slab due to continuous fluid releases (Cameron et al., 2003; Ryan and Chauvel, 2014). If Cretaceous basaltic magmatism in the NCC was associated with the Paleo-Pacific plate subduction, similar decreasing trends of fluid mobile elements along the subduction direction are also expected.

In principle, the involvement of recycled lower continental crust through delamination may also reconcile "arc-like" geochemical characteristics with very low $\varepsilon_{Nd}(t)$ of some > 108 Ma basalts, because ancient cratonic continental crust usually has lower $\varepsilon_{Nd}(t)$ than typical arc basalts (Clift et al., 2009; Kelemen et al., 2003; Xu, 2001; H.F. Zhang et al., 2008). Partial melting of the lithospheric mantle metasomatized by felsic melts derived from crustal eclogite with rutile residual can also well explain low Nb content, high Nb/Ta and "island arc-like" trace element distribution patterns of those > 108 Ma basalts from Fangcheng, Feixian, Shihetun and Yixian (Liu et al., 2008; Yang et al., 2008; H.F. Zhang et al., 2002, 2003). In addition, the enriched lithospheric mantle source for the > 108 Ma alkali basalts may also be formed through interactions between the refractory old lithospheric mantle with melts from the subducted ancient continental crust (H.F. Zhang et al., 2003). For example, the isotopic compositions of the Fangcheng basalts can be well explained by the involvement of crustal components from the subducted Yangtze block into the old lithospheric mantle (Guo et al., 2013; Zhang et al., 2002). However, since both ancient continental crust and cratonic lithospheric mantle are dry, the subducted ancient continental crust cannot provide sufficient water to produce hydrous basaltic magmas (Guo et al., 2013). In fact, there is increasing evidence that the mantle sources of the > 108 Ma alkali basalts beneath the NCC are wet. To be specific, recent studies revealed that the lithospheric mantle beneath the NCC was hydrous (> 1000 ppm) at ~125 Ma (Fig. 5), which is significantly higher than H_2O contents of the lithospheric mantle in the Late Cretaceous and the Cenozoic (Guo et al., 2013; Li et al., 2015; Xia et al., 2013a, 2013b; Yang et al., 2008). The estimated water contents of ~119 Ma primitive basaltic magmas can even reach the level of modern island arc basalts (Xia et al., 2013b). The major element variations may also reflect the high H_2O contents in the > 108 Ma alkali basalts. As shown in Fig. 5, the > 108 Ma alkali basalts show small changes in FeO and TiO_2 contents with increasing FeO/MgO. Since FeO and TiO_2 are rejected by plagioclase, fractionation of plagioclase causes significant increase of FeO and TiO_2 contents in residual magma (Albarède, 2003). In contrast, when plagioclase are undersaturated, fractionation of mafic minerals will lead to significant increase in FeO/MgO but small changes in FeO and TiO_2 contents. Previous studies demonstrated that plagioclase undersaturation can be obtained by either high-pressure fractionation (OIB) or high water activity in the magmatic sources (arc magma) (e.g. Albarède, 2003; Asimow and Langmuir, 2003). Interestingly, the "OIB-like" < 108 Ma alkali basalts show a trend of plagioclase fractionation, but there is no such trend for the "arc-like" > 108 Ma alkali basalts. Although the < 108 Ma Cretaceous alkali basalts may have derived from shallower depth than the > 108 Ma alkali basalts due to lithosphere thinning, the lithosphere is still thicker than 30 km (in fact, > 60 km), where the minimum melt of mantle rocks is saturated in olivine, spinel and clinopyroxene but not plagioclase (Presnall et al., 1978). Therefore, the observed fractionation crystallization trend of plagioclase for the < 108 Ma Cretaceous alkali basalts occurred at lower pressure, where magma might have already reached shallower depths. In contrast, such a fractionation process of plagioclase in shallower depth didn't occur for the > 108 Ma alkali basalts. In this regard, the lack of major element variations associated with plagioclase fractionation for the > 108 Ma alkali basalts was most likely resulted from high H_2O activity in these basaltic magmas.

The high H_2O contents strongly suggest the involvement of plate subduction (Ling et al., 2013; Niu, 2005; Sun et al., 2007), and thus the role of the subducting Paleo-Pacific plate in modifying the old lithospheric mantle should also be considered. During plate subduction, fluid mobile elements are transferred from subducting slabs to the overlying mantle in forms of various combinations of hydrous fluids, silicate melts and supercritical fluids (Bebout, 2014). Thus the metasomatized mantle source would be variably enriched in fluid mobile elements (e.g. Ba, Sr, Rb, K and Pb) (Fitton et al., 1988, 1991; Hawkesworth et al., 1984; McDonough, 1991). The involvement of subduction contributions is further illustrated in Fig. 6, which shows positive correlations between K_2O/TiO_2 and Ba/Zr for the > 108 Ma alkali basalts, as well as Pb/Zr versus Ba/Zr. Since Ba, Pb and K are all fluid mobile elements, this phenomenon may be plausibly explained by addition of fluids from subducting oceanic slabs (Ormerod et al., 1988).

Interestingly, some fluid mobile/immobile element ratios are geographically related, i.e., there is an increasing trend between Ba/Zr and $(Th/Nb)_N$ for basalts from Jining, Chengde and Xishan in the west, to Sihetun and Feixian in the east, while basalts from Fangcheng are out of this trend with relatively higher $(Th/Nb)_N$ (Fig. 7). One may argue that some of these ratios, such as Ba/Zr, Pb/Zr and K_2O/TiO_2, are partly associated with fractionation crystallization processes. So the geographic changes are also examined by some incompatible trace element pairs. Consistently, La/Nb increases, whereas Nb/U decreases with increasing $(Th/Nb)_N$ from west (Jining, Chengde and Xishan) to east (Sihetun, Fangcheng and Feixian) (Fig. 8). Ratios of incompatible elements with similar geochemical behavior, such as Nb/U, Th/Nb and La/Nb, do not fractionate significantly during partial melting and crystal fractionation processes, and thus are good index to trace mantle source signatures (Hofmann, 2003; Sun et al., 2008). However, these element pairs are fractionated from each other during dehydration and metasomatism processes in subduction zones (Guo et al., 2014; Niu and O'Hara, 2003; Sun et al., 2008). The Th/Nb is even viewed as a sensitive index of slab additions (Elliott et al., 1997; Kelemen et al., 2003; Turner and Langmuir, 2015). Previous studies also showed that primitive arc magmas are characterized by $(Th/Nb)_N > 1$, while MORB and OIB have $(Th/Nb)_N < 1$ (Hofmann, 1997; Niu and O'Hara, 2003; Sun and McDonough, 1989). Meanwhile, thorium behaves as an immobile HFSE in aqueous fluids (Keppler, 1996; Turner and Hawkesworth, 1997), so Th enrichment in arc magma is generally ascribed to melt additions from subducting sediments or basalts in eclogite facies with residual rutile (Kelemen et al., 2003; Sun et al., 2004). As mentioned above, the metasomatized mantle wedge containing high proportions of H_2O-rich components produces arc-related magma with high fluid mobile element contents and mobile/immobile element ratios (Reiners et al., 2000; Ryan and Chauvel, 2014; Stolper and Newman, 1994). Then, if we adopt these ratios to evaluate amounts of recycled crustal materials in their mantle sources, the decreasing Th/Nb and La/Nb ratios, but increasing Nb/U from the east to the west reflect decreasing subduction additions to the lithospheric mantle of the NCC during the Early Cretaceous. Although the "arc-like" geochemical features are possibly associated with any ancient subduction events, such as the northward subduction of the Tethyan before the South-North China collision and the Paleo-Asian oceanic subduction along the north margin of the NCC, the northwestward declining "arc signatures" strongly emphasized the role of the westward subduction of the Paleo-Pacific plate in lithosphere metasomatism.

Although basalts from Liaodong region (the Xiaoling basalts), which is closer to the subduction zone than other sites in the NCC (Fig. 1), do

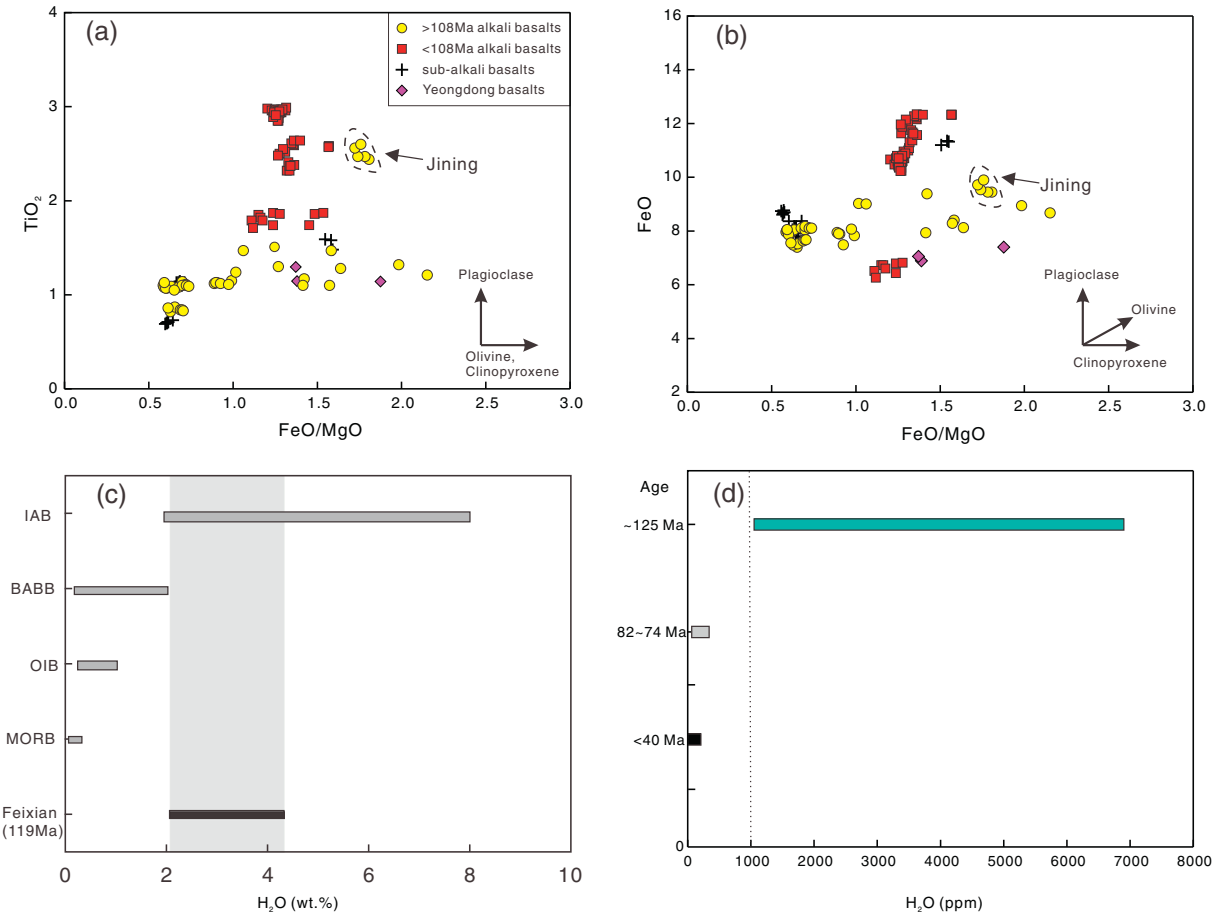

Fig. 5. Plots showing high H_2O contents of > 108 Ma alkali basalts and their mantle sources. (a) and (b) demonstrate the fractional crystallization trend of plagioclase for the > 108 Ma alkali basalts. (c) Water contents of different magmas to show high H_2O contents of the ~119 Ma Feixian basalts Xia et al. (2013b). (d) Water content variations of lithospheric mantle beneath the North China Craton. Data are from Xia et al. (2013b), Li et al. (2015), Yang et al. (2008), Bonadiman et al. (2009) and Xia et al. (2010).

not exhibit the highest La/Nb and Th/Nb, and the lowest Nb/U (Fig. 8), they still have higher LILE and lower HFSE than the OIB-like Jining basalts. Their isotopic compositions also indicate that less recycled crustal components are incorporated into the magma source of the Xiaoling basalts through subduction metasomatism. As shown it Fig. 2, the Xiaoling basalts have comparable ε_{Nd} (t) to basalts from Fangcheng, Feixian and Yeongdong basin, but they also display much lower initial $^{87}Sr/^{86}Sr$. The relatively weak "arc signatures" of the Xiaoling basalts is not surprising, because the Xiaoling basalts erupted around 110 Ma (Pang et al., 2015), which is younger than other > 108 Ma alkali basalts but close to the timing of major transition in basalt compositions.

Geochemical characteristics suggest that the Jining basalts are devoid of significant fluid metasomatism in their mantle source due to the long distance from the subduction zone. Instead of slab-derived fluids/melts, the main metasomatic agent is suggested to be melts generated by partial melting of the dehydrated oceanic slab (Guo et al., 2014). The main trigger for partial melting was probably heat supplied from asthenosphere disturbed by slab rollback. The temperature is hot enough to melt rutile, such that no HFSE depletion is observed.

Therefore, the northwestward decreasing trend of subducting "signals", changing from "arc-like" magmas to "OIB-like" magmas (Jining basalts) is probably related to the northwestward subduction of the Paleo-Pacific plate. This is also supported by spatial distributions of the > 108 Ma basalts, e.g., sub-alkali basalts are distributed in regions nearer to subduction zone than alkali basalts (Fig. 1).

4.2. Enriched components in the < 108 Ma Cretaceous alkali basalts

As shown above, the < 108 Ma Cretaceous alkali basalts are characterized by OIB-like geochemical compositions. The depleted Sr-Nd isotopic composition and OIB-like trace element patterns can be attributed to contributions from asthenosphere, likely through formation and melting of pyroxenite (Gao et al., 2008; Liu et al., 2008). However, these basalts have slightly enriched fluid mobile elements (e.g. Ba, Pb and Sr) relative to typical OIB (Fig. 4), which may relate to subduction enrichments. This conclusion is supported by positive correlations between fluid mobile elements to HFSE ratio pairs and Ba/Zr versus $(Th/Nb)_N$ for alkali basalts from Fushun, Fuxin and Niutoushan (Figs. 6 and 7c). Some < 108 Ma Cretaceous alkali basalts even display similar Pb/Zr and Ba/Zr with arc basalts (Fig. 6c).

It is also noteworthy that alkali basalts from Fuxin (Jianguo) have higher K_2O/TiO_2, Ba/Zr and Pb/Zr than that from Qujiatun region, although the Fuxin basalts have lower $(Th/Nb)_N$ (Fig. 7c). If the $(Th/Nb)_N$ is viewed as an index to trace contributions from aqueous melt metasomatism, the higher fluid mobile element to HFSE ratios of the Fuxin (Jianguo) basalts indicate that apart from primary contributions from asthenosphere, the involved enriched components in the relict old lithospheric mantle may contain more contributions from fluid metasomatism. In summary, the primary source of the < 108 Ma Cretaceous alkali basalts is asthenosphere, but these asthenosphere-derived melts were be "contaminated" by varying proportion of slab-derived components in the overlying relict old lithospheric mantle.

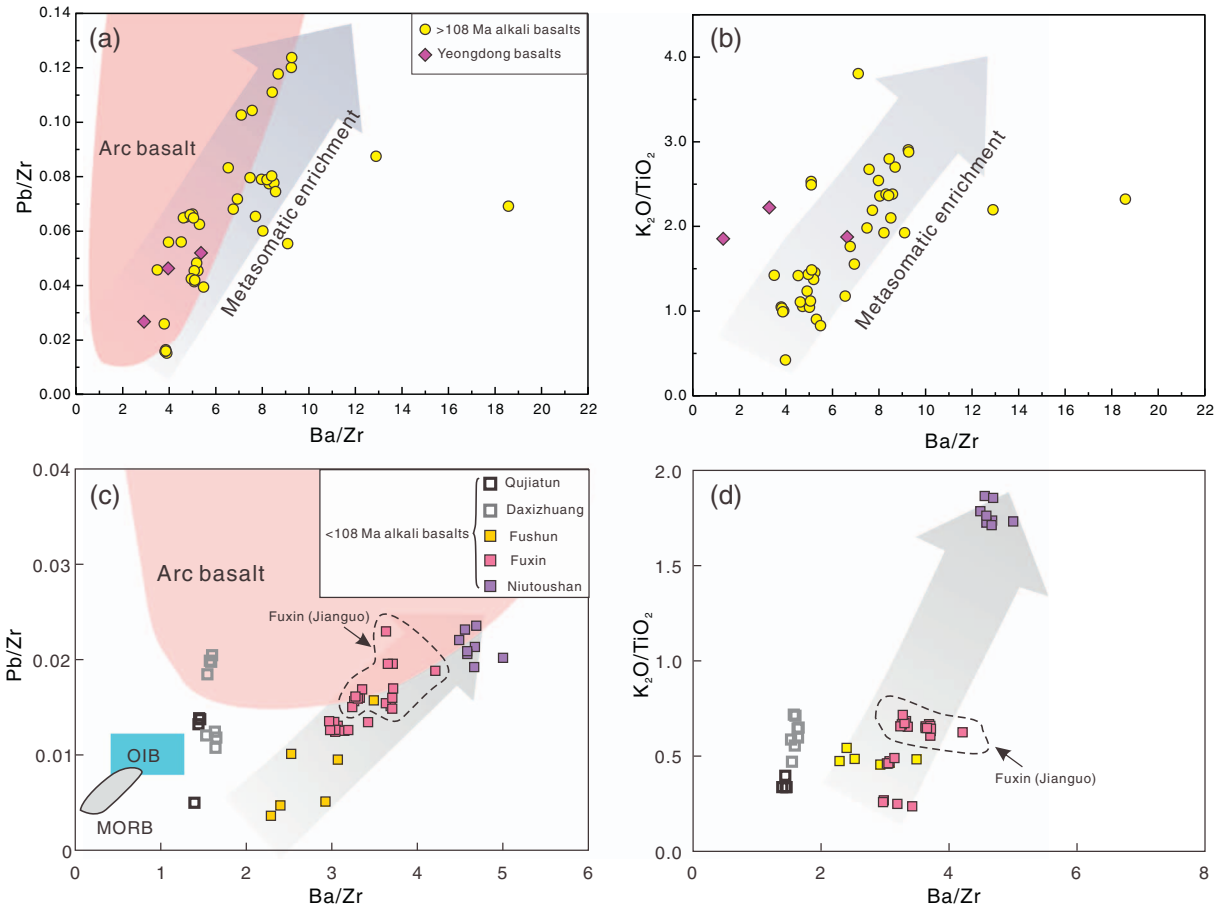

Fig. 6. Fluid mobile element to HFSE ratios versus Ba/Zr for the > 108 Ma alkali basalts from NCC to identify clues for fluid metasomatism. Data for the field of arc basalt are from Kelemen et al. (2003) and GEOROC: http://georoc.mpch-mainz.gwdg.de/georoc/. MORB and OIB fields are from Sun and McDonough (1989), Weaver (1991) and Hart et al. (1992).

4.3. Ridge subduction and Cretaceous basaltic magmatism

4.3.1. Flat subduction of the spreading ridge between the Pacific and Izanagi plates

From the above discussion, the northwestward subduction of the Paleo-Pacific plate (Izanagi and Pacific) may be responsible for the formation of Cretaceous alkali basalts. Seismic studies indicated that the subducted Pacific slab stagnated in the mantle transition zone can subhorizontally reach the North-South Gravity Lineament (Huang and Zhao, 2006), which is about 2000 km far from the Japan Trench (Yang et al., 2012). The amount of the stagnated slab matches well with those subducted during the Cenozoic, and earlier subduction records, namely "the Izanagi plate related heterogeneity" in the lower mantle, have also been observed (Li et al., 2013; Li and Yuen, 2014). Normal subduction is not likely to impose major influence on regions > 800 km inland from the subduction zone (Jordán et al., 1983; Li and Li, 2007). In contrast, ridge subduction often reaches far inland through flat subduction (Sun et al., 2010).

Flat subduction refers to those subducting oceanic plate with shallow or horizontal subduction angles beneath the overriding plate (Antonijevic et al., 2015; Li and Li, 2007; Ramos et al., 2002). Recent geophysical observations in the South America showed that the flat slab is the shallowest to the surface along the present-day projected location of ridge, while slabs on both sides of the subducting ridge change abruptly from flat to normal (Antonijevic et al., 2015).

There is increasing evidence that a flatly subducting ridge has been continuously moving northward along the eastern Asian continental margin from the Jurassic to the Cenozoic (Kinoshita, 1995; Ling et al., 2013; Sakaguchi, 1996; Sun et al., 2007). The presence of the northwestward younging sequence of magnetic lineations in the northwest Pacific seafloor indicated that a ridge subducted under eastern Asian continental margin at some time in the past (Straub et al., 2009; Seton et al., 2012). During the Late Jurassic to the Cretaceous, two oceanic plates were located to the east of eastern Asian continental margin with the Pacific plate in the south and the Izanagi plate in the north (Maruyama et al., 1997; Sun et al., 2007; Ling et al., 2009). Combined with the drifting history of the Pacific and the Izanagi plates and linearly distributed adakites, A-type granites, Nb-enriched basalts and Cu-Au deposits, the spreading ridge has been suggested to be located at the Lower Yangtze River belt at ~140 Ma (Li et al., 2011; H. Li et al., 2012; Ling et al., 2013). Similar rock assemblage, especially linearly distributed adakites (130 ± 5 Ma) with arc-shaped nappe structures in the Shandong peninsula and the Xu-Huai region, indicated that the ridge moved to the Shandong Peninsula at ~130 Ma (Ling et al., 2013; Li et al., 2014). Meanwhile, it has also been suggested that there was a pulse of heat flow anomalies (up to ~80 mW/m^2) in the Early Cretaceous (130–110 Ma) (Menzies et al., 2007). In addition, ridge subduction records in the Late Cretaceous-early Cenozoic are well preserved in adjacent regions, e.g., pulses of volcanism and anomalous heat flow in Japan and Korea (Kinoshita, 1995; Sagong et al., 2005; Sakaguchi, 1996). Therefore, flat subduction of the nowaday "extinct" spreading ridge between the Izanagi plate and the Pacific plate are the best option to reconcile these issues.

4.3.2. Ridge subduction and spatial-temporal evolution of Cretaceous basalts

Based on above observations, we propose a mechanism to link up ridge subduction with Cretaceous basaltic magmatism in the NCC. The

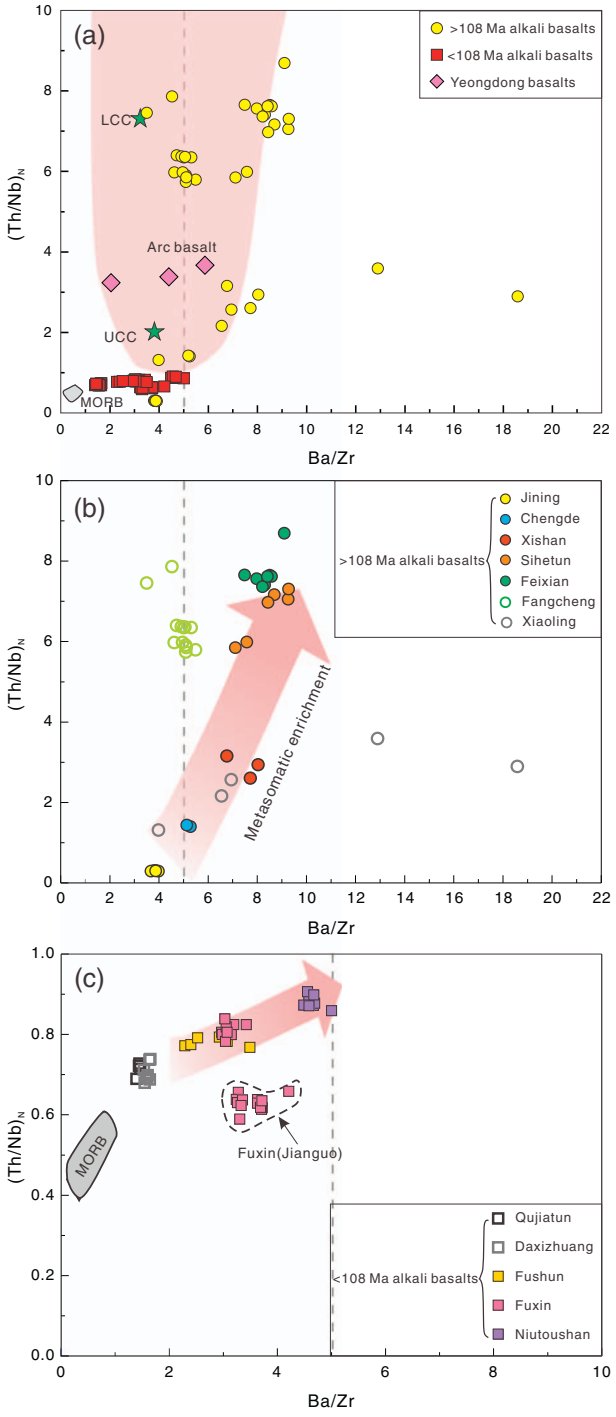

Fig. 7. Ba/Zr versus $(Th/Nb)_N$ diagrams for Cretaceous alkali basalts in the North China Craton. Data for field of arc basalt are from Kelemen et al. (2003) and GEOROC: http://georoc.mpch-mainz.gwdg.de/georoc/. MORB and OIB fields are from Sun and McDonough (1989) and Weaver (1991). LCC and UCC represent the lower continental crust and the upper continental crust, respectively.

ridge subduction started at ~130 Ma slightly to the south of the Shandong Peninsula (Ling et al., 2013). This subducting ridge reached far inland such that H_2O-rich components released by slabs on both sides metasomatized the overlying lithospheric mantle and possibly convective mantle wedge. These metasomatism "signals" were eventually imprinted in Cretaceous basalts erupted on the surface, where "arc-like" basalts would distribute as a "parabola" (Fig. 9).

Relationships between Cretaceous basaltic magmatism in the NCC and drifting history of the spreading ridge between the Pacific plate and the Izanagi plate are further illustrated in Fig. 10. The ridge was subducting towards the Xuhuai region at ~130 Ma, as inferred from linear distribution of slab-melting derived adakites and A-type granites in Xuhuai region and the Shandong Peninsula (Li et al., 2014; Ling et al., 2013). Partial melting of the lithospheric mantle metasomatized by slab-derived components from the Izanagi plate produced Xishan basalts at this time. Considering that the northward drifting rate of the Izanagi plate was faster (Maruyama et al., 1997; Sun et al., 2007), the spreading ridge would move to the north. Fangcheng, Feixian, Sihetun and Yixian were situated on "flanks" of the "parabola" around 125 Ma, resulting in "arc-like" basaltic magmatism in these regions (Fig. 10b). Meanwhile, the drifting direction of the Pacific plate turned to northwest around 125 Ma (Sun et al., 2007), which accelerated the northward drifting of the "extinct" ridge (Ling et al., 2013; Ling et al., 2009; Sun et al., 2010). When the Chengde basalts erupted, the flat subduction ridge was probably located to the north of the Bohai Gulf (Fig. 10). So enriched components in the mantle source of Chengde basalts (114 Ma) were largely controlled by the subducting Pacific plate. Jining was far away from the subduction zone, which might be out of subduction dehydration affected regions. Instead of H_2O-rich components from the subducted slabs, melts derived from the dehydrated slab may act as the predominant metasomatic agent (Guo et al., 2014). Mantle flow induced by continuous slab rollback may be the trigger for partial melting of its mantle source. These plausibly explain the relatively long-lasting basaltic magmatism (119.6–108.6 Ma) and its OIB-like geochemical characteristics. Distributions of Cretaceous basalts is also in favor of the slab rollback process. The > 108 Ma basalts develop even in the west block of NCC, while the < 108 Ma Cretaceous basalts are only distributed in regions adjacent to the Tan-Lu fault and the Korean peninsula (Fig. 1), indicating that basaltic magmatism in the NCC migrated from the west to the east in the Cretaceous.

With continuously northward drifting and/or slab rollback, the flat subduction ridge left the NCC at ~108 Ma (Fig. 10c). Enriched components in the mantle source of the Xiaoling basalts (110 Ma) were also largely related to the subducting Pacific plate but less recycled crustal materials were involved. In contrast, Fuxin and Niutoushan were out of the "parabola" at this time (Fig. 10c), where the flat-subduction ridge was no longer acting as a physical barrier beneath the subcontinental lithospheric mantle. Northward moving away of the flatly subducting ridge and/or slab rollback triggered decompression melting of upwelled asthenosphere. Then, asthenosphere-derived melts were involved in generating the Fuxin and Niutoushan "OIB-like" basalts. Meanwhile, these melts may interact with overlying lithospheric mantle, which was previously metasomatized by slab-derived components. In this case, basalts may inherit some subduction "signals". This feasibly explains why the < 108 Ma Cretaceous alkali basalts are also relatively enriched in fluid mobile elements than typical OIB.

Locations of the spreading ridge between the Pacific and the Izanagi plates after 100 Ma have been well constrained using volcanic pulse and anomalous heat flow observed in southwest Japan, e.g., the estimated geothermal gradient of Cretaceous stratigraphic units was > 90 °C, indicating the opening of slab window (Sakaguchi, 1996). The northward younging age trend of granites along the Median Tectonic Line in southwest Japan also recorded the ridge subduction event (Kinoshita, 1995). Around 80 Ma, the ridge intersected with the north part of Cretaceous Shimanto Belt (Kinoshita, 1995). The Fuxin basalts (106.1 Ma) and the Niutoushan basalts (107–94 Ma) are relatively older and located closer to the subduction affected regions than other < 108 Ma alkali basalts (Fig. 10c and d), and thus inherited more subduction signatures, as suggested by relatively higher Ba/Zr and Pb/Zr than other < 108 Ma alkali basalts. It is also noteworthy that alkali basalts from Yeongdong basin around 80 Ma still have arc-like geochemical characteristics. This is because Yeongdong basin was close to the Cretaceous subduction zone.

Such a ridge subduction event is also consistent with stress field changes in the NCC. The North China Craton experienced episodic

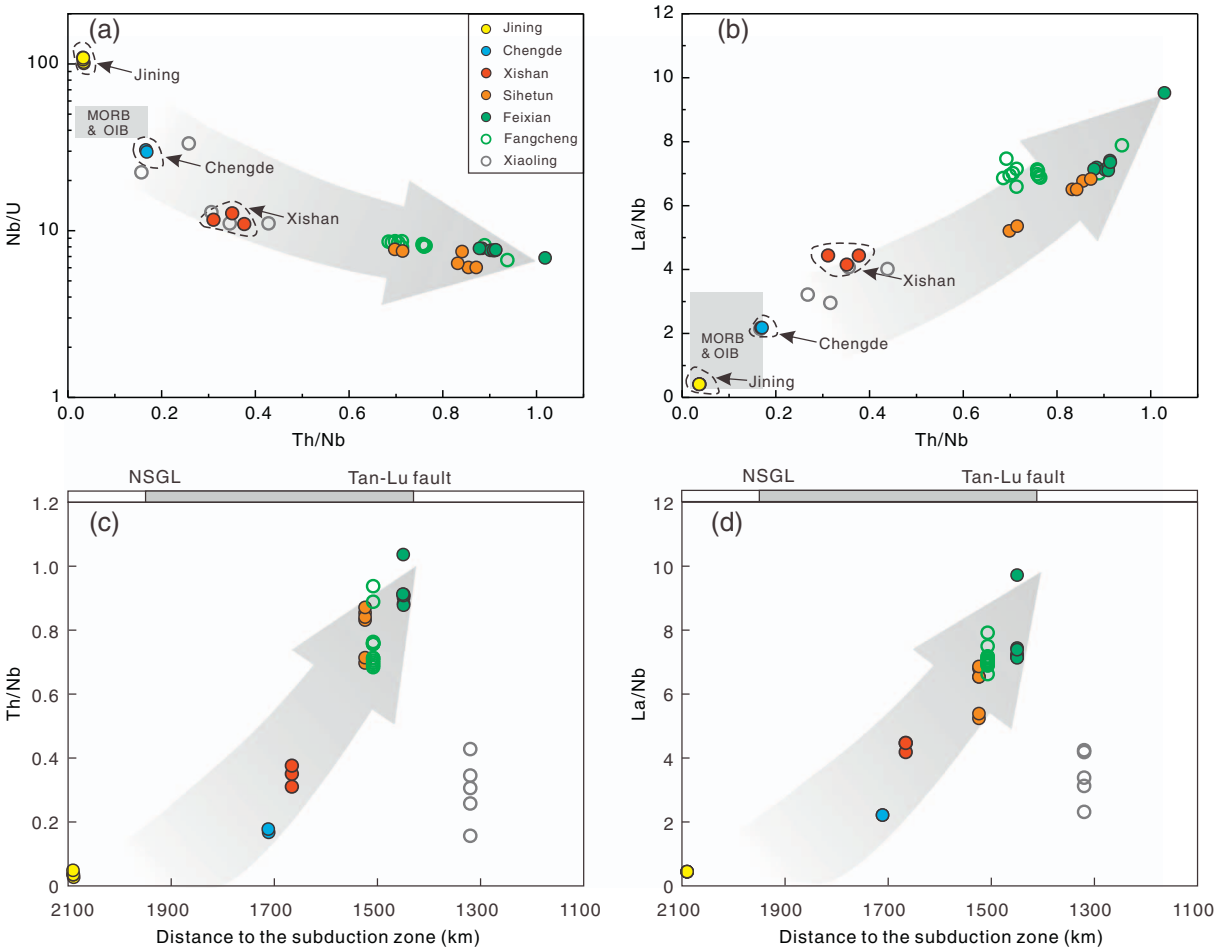

Fig. 8. (a) Nb/U versus Th/Nb, (b) La/Nb versus Th/Nb diagrams for the > 108 Ma alkali basalts in the NCC. The "MORB & OIB" fields are from Hofmann (2003). (c) and (d) Th/Nb and La/Nb versus distance to the subduction zone for each basalt intrusion. NSGL is the North-South Gravity Lineament.

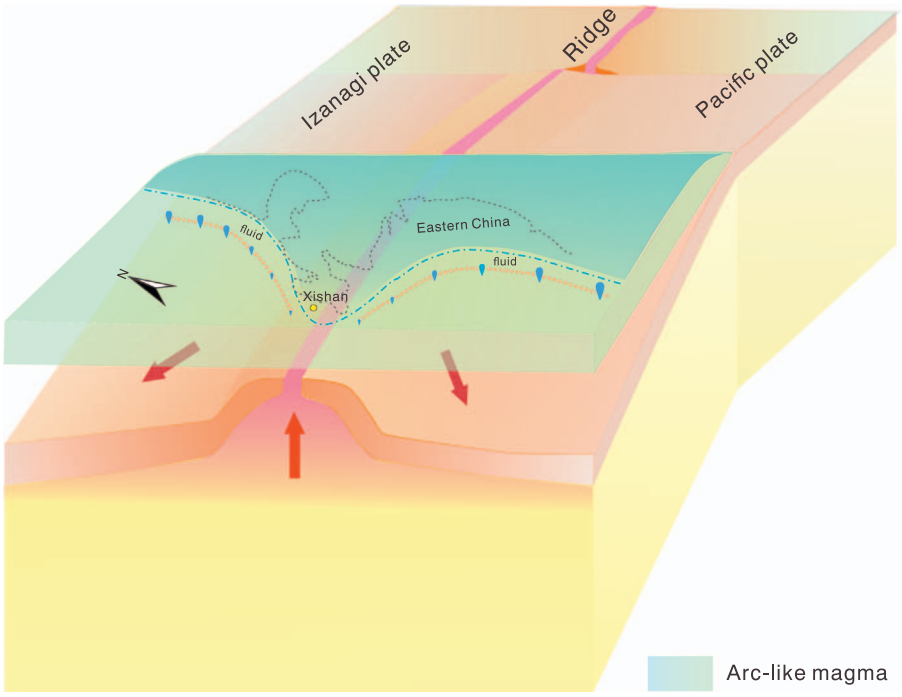

Fig. 9. Schematic carton illustrating relationships between Cretaceous basaltic magmatism and the westward subduction of the Paleo Pacific at ~130 Ma. The blue dash line refers to furthest boundary with significant subducting dehydration metasomatism, as indicated by occurrence of "arc-like" magma on the surface. (For interpretation of the references to color in this figure legend, the reader is referred to the web version of this article.)

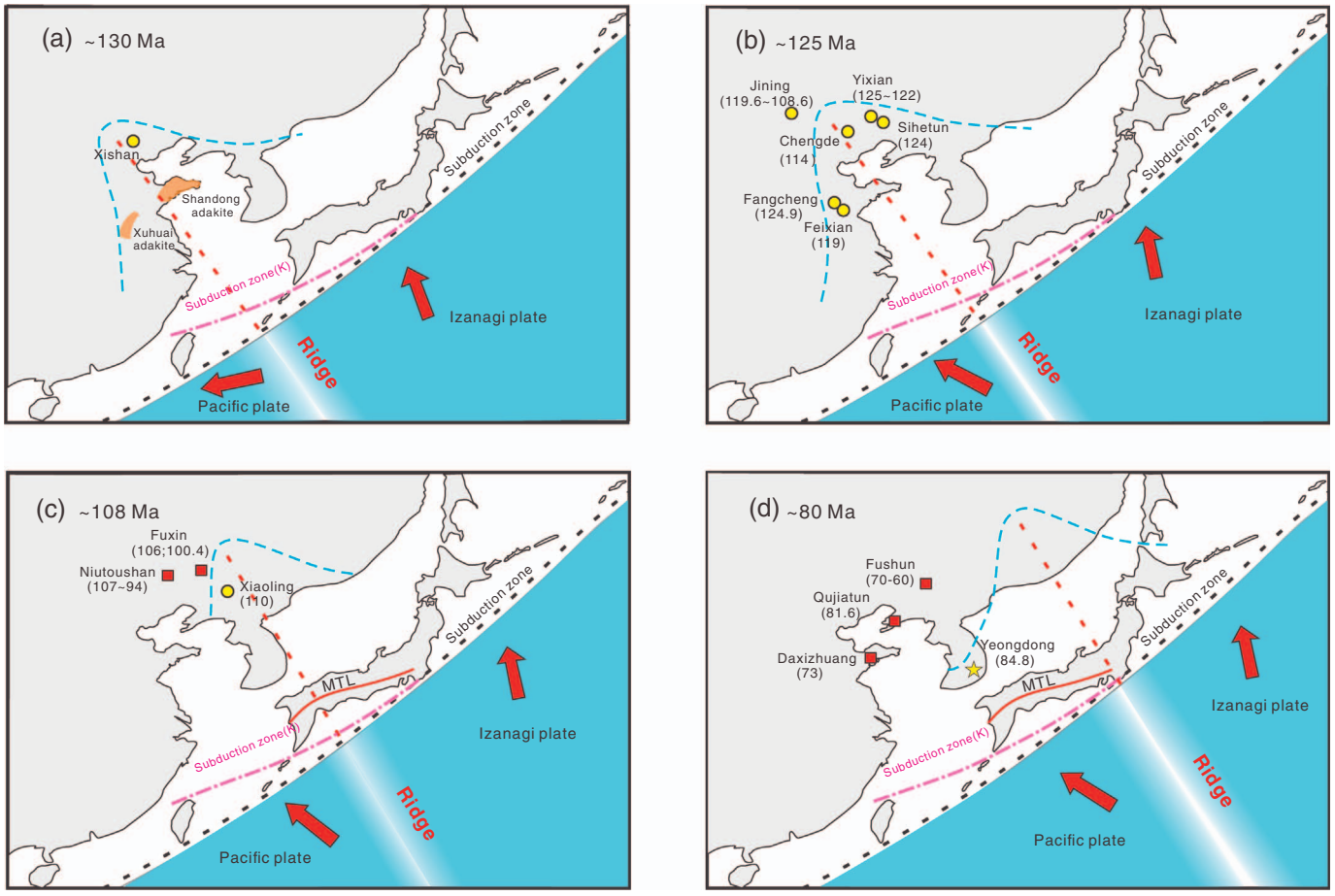

Fig. 10. Relationships between alkali basaltic magmatism in the NCC and drifting history of the mid-oceanic ridge between the Pacific plate and the Izanagi plate along the East Asia. Field of adakites formed about 130 Ma is after Ling et al. (2013). MTL represents the Median Tectonic Line in Japan. The age trend of granites along MTL indicates ridge subduction processes during the late Cretaceous (Kinoshita, 1995). The purple dashed line represents the locations of subduction zone in the Cretaceous, which is after Sengör and Natal'in (1996). Drifting direction of the Pacific and the Izanagi plates is from Sun et al. (2007). (For interpretation of the references to color in this figure legend, the reader is referred to the web version of this article.)

continental-scale compressional and extensional tectonic events from the Late Jurassic to the Cenozoic (Lin et al., 2013a and references therein; Zhao et al., 2004; Davis et al., 2001). It is widely accepted that the compressional deformation occurred during the Late Jurassic to the Early Cretaceous (Lin et al., 2013a and references therein), which was then followed by widespread late Early Cretaceous to Eocene extensional structures and metamorphic core complexes (Lin et al., 2013b and references therein). However, localized compressional deformation and tectonic inversions also occurred in the Cretaceous. For example, in the late Early Cretaceous (from ~125–122 Ma to ~110 Ma), the stress field along the Tan-Lu fault changed from extension to southeast-northwestward transpression, and magmatism in previously formed extensional basins ceased at ~125 Ma (Wang et al., 2006, 2007; Y.Q. Zhang et al., 2003; Sun et al., 2007), which is slightly different from the core of the NCC, due to varied influences from the Pacific and Izanagi plates. In addition, the Jiaolai basin in Shandong peninsula experienced a tectonic reversion from extensional to compressional deformation during the Aptian (~120 Ma) (Y.Q. Zhang et al., 2008), which resulted in large scale gold mineralization (Sun et al., 2007, 2013). Additionally, the Yunmengshan metamorphic core complex was subjected to large-scale uplifting during 125–114 Ma and magmatism ceased (Chen et al., 2014), when the flatly subducted ridge passed through the Shandong peninsula and regions adjacent to the Bohai Gulf. Since the northward moving of the flatly subducting ridge was accompanied by continuous slab rollback of the Pale-Pacific plate, only regional compression or transpression occurred. In contrast, after northward moving away of the flatly subducting ridge, the NCC experienced regional back-arc extension due to continuous slab rollback, and there developed many sedimentary basins in eastern China during the Late Cretaceous and the Cenozoic (Ren et al., 2002; S.Z. Li et al., 2012).

4.4. Implications for the destruction of the NCC

Although destruction of the NCC has been recognized for at least three decades (Fan and Menzies, 1992; Menzies et al., 2007; Xu, 2014; Zhu et al., 2012b), deep-level processes of lithosphere thinning are still under hot debate. No mechanism for lithospheric destruction is well agreed because of inability to interpret some specific problems (Gao et al., 2008; Ling et al., 2013; Menzies et al., 2007; Niu, 2005; Xu, 2001). The delamination model suggests that lower crustal eclogite was delaminated into convective mantle in the Jurassic due to its higher density than peridotite (Gao et al., 2002; Gao et al., 2004; Wu et al., 2002). Recycled lower crustal eclogite was then involved in generating the Early Cretaceous basalts and high-Mg adakites (Gao et al., 2008; Liu et al., 2008). Meanwhile, delamination of the lithospheric mantle and the lower crust also caused asthenosphere upwelling, which may directly contact with the lower crust resulting in large scale crustal melting within 10 Ma (131–117 Ma) in eastern China (Wu et al., 2005). The rapid delamination model was questioned for unable to explain how buoyant refractory lower lithospheric mantle (3.30–3.32 g/cm^3) was converted to a fertile denser one (> 3.34 g/cm^3) (Menzies et al., 2007). Meanwhile, this model also failed to explain why lithospheric

mantle-derived magmatism lasted for a prolonged time (180–90 Ma) and why there is no voluminous asthenosphere-derived magmatism shortly after the "quick delamination" event (Ling et al., 2013; Menzies et al., 2007; Xu et al., 2004). In addition, using the discrimination diagram of Liu et al. (2010), most of the NCC adakites belongs to slab melts (Ling et al., 2013).

Thermal erosion model argued that the lithospheric mantle-derived magmatism lasted from ~180 to 90 Ma, which corresponded to a prolonged melt-rock reaction process that transformed the refractory lithospheric mantle into a fertile one (Menzies et al., 2007; Xu, 2001; Xu et al., 2004; H.F. Zhang et al., 2003). Moreover, recycled upper and lower oceanic crust are also recently recognized only in a few 90–40 Ma basalts to support the protracted lithosphere thinning process, because fusible recycled crust may experience a large degree of melting and cause vast contemporary magmatism if the lithosphere was already very thin (Xu, 2014). The thermal erosion model requires volumes of mafic melts over a long period of time to transform the > 100 km refractory ancient lithospheric mantle (Ling et al., 2013; Menzies et al., 2007). However, even though the Kaapvaal craton has been overriding the African super plume (Burke et al., 2008; Ni et al., 2002), it still remains stable. Meanwhile, this model also fails to explain why lower continental crust-derived magma occurred prior to large-scale basaltic magmatism (Gao et al., 2004, 2008). The lithosphere hydration model encountered difficulties in explaining two questions: (1) how much water was available in recycled slabs (Menzies et al., 2007); (2) the NCC experienced several subduction and collision events, but why hydration of the lithospheric mantle happened in the Late Mesozoic and only related to the westward subduction of the Paleo-Pacific plate (Ling et al., 2013).

The ridge subduction model provides a dynamic trigger of lithosphere thinning, which can not only explain the spatial distribution and isotopic characteristics of the Cretaceous adakites and A-type granite in the NCC (Li et al., 2014; Ling et al., 2013), but also offer a possible way to reconcile those issues mentioned above. The most intense period of the lithosphere thinning was the Early Cretaceous (Xu et al., 2004), when the "extinct" ridge was located at the center of the NCC and may reach far inland through flat subduction (Ling et al., 2013). The influence of ridge flat subduction on the destruction of the NCC is embodied in two aspects: reducing the viscosity of the lithospheric mantle by successive fluid/melt injection and imposing regional lateral forces on the lithospheric mantle through flat subduction (Ling et al., 2013; Saunders et al., 1992; Windley et al., 2010; Xia et al., 2013b). Such voluminous fluid/melt injection and metasomatism hydrated and enriched the ancient lithospheric mantle in the Early Cretaceous. For example, the > 108 Ma alkali basalts were generated by partial melting of the ancient lithospheric mantle enriched by H_2O-rich components from slabs on both sides of the flatly subducting ridge. Meanwhile, flat subduction may not only laterally erode the overlying cratonic lithosphere (subduction erosion) (Zhang et al., 2009; Zheng and Wu, 2009), but also impose a lateral force to drive thickening and delamination of the ancient lithospheric mantle at the initial stage along the East Asia continental margin. This can plausibly explain why the foundered lower crust-derived Cretaceous adakitic rocks occurred earlier than basaltic magmatism in the NCC.

Temporal evolution of mantle lithosphere composition is also consistent with our flat subduction model. Basalts and mantle xenoliths make it possible to explore how the ancient refractory lithosphere mantle became enriched in the Early Cretaceous and then evolved into the Cenozoic fertile lithospheric mantle with depleted isotopic compositions. The garnet and spinel peridotite xenoliths in Ordovician kimberlites have variable initial $^{87}Sr/^{86}Sr$ (t = 125 Ma) ratios (0.7045–0.7199) and $\varepsilon_{Nd}(t)$ from − 2 to − 9 (Fig. 2) (H.F. Zhang et al., 2008; Zhang and Yang, 2007). Meanwhile, presence of pyroxenite xenoliths with lower $\varepsilon_{Nd}(t)$ (− 21) and moderate $(^{87}Sr/^{86}Sr)_i$ (0.705923) in these kimberlites emphasizes the isotopic heterogeneity of the ancient lithospheric mantle. Therefore, enriched isotopic composition of the > 108 Ma alkali basalts can be interpreted by the lithospheric mantle heterogeneity. However, high LILE and LREE contents of these basalts cannot be generated by partial melting of the refractory ancient lithospheric mantle (Zhang, 2005). Taking the Jining basalts for example, negative $\varepsilon_{Nd}(t)$ suggests primary contributions from the ancient lithospheric mantle, but they have lower LILE and LREE contents than other > 108 Ma alkali basalts due to less recycled crustal components. In principle, recycling of crustal materials induced by all subduction and collision events along craton margins may contribute to generate the LILE and LREE enriched lithospheric mantle. However, the northwestward decreasing extent of fluid mobile element enrichment, together with spatial distribution of alkali basalts and sub-alkali basalts, indicates that the metasomatized lithospheric mantle may be largely controlled by the westward subduction of the Paleo-Pacific plate. Previous subduction-induced trace element enrichment may also exist, but it might be overprinted or intensively modified by such a westward flat subduction event.

The recently reported lamprophyres and diabase-porphyries (123–121 Ma) have high LREE concentrations (similar to contemporary arc-like lamprophyres) and OIB-like geochemical characteristics (no depletion of HFSE and negative Pb anomalies), but they also exhibit a wide range of $\varepsilon_{Nd}(t)$ and $\varepsilon_{Hf}(t)$ from positive to negative (Dai et al., 2016; Ma et al., 2014, 2016). These geochemical features can be ascribed to partial melting of the lithospheric mantle recently metasomatized by small melt fractions with high LREE and depleted Nd-Hf isotopic compositions, which are formed during asthenosphere upwelling associated with the opening of a slab window (Beard and Johnson, 1997; Farmer et al., 1995). Such a scenario was also suggested to occur in the western US, Antarctic Peninsula and British Columbia (Beard and Johnson, 1997; Farmer, 2014; Hole et al., 1991). Similarly, these mafic dykes in Shandong peninsula may derive from the newly accreted lithospheric mantle metasomatized by small volume melts associated with the opening of slab window. This can plausibly explain why contemporary basaltic magmatism in the NCC was still characterized by "arc-like" geochemical compositions. Meanwhile, heat supplied from the upwelled asthenosphere within the opening slab window may contribute to the large scale crustal melting in Shandong peninsula, Liaodong and Liaoxi regions during the Cretaceous.

The contrasting geochemical characteristics between the > 108 Ma and the < 108 Ma Cretaceous basalts reflect a transition in deep-level processes, when lithosphere hydration and lateral erosion related to the flatly subducting ridge was replaced by thermal erosion and melt-rock reaction associated with asthenosphere upwelling. Specifically, with continuous slab rollback and northward moving away of the flatly subducted ridge from the NCC around 108 Ma, the oceanic lithosphere would no longer act as a physical barrier so that the disturbed asthenosphere can directly interact with the relict old lithospheric mantle. In contrast to small volume melts from the opening slab window at Shandong peninsula during the Early Cretaceous, decompression melting of the upwelled asthenosphere produced large amounts of melts with depleted isotopic compositions. Successive melt injections from asthenosphere gradually diluted/washed out subduction "signals" of the overlying lithospheric mantle, and probably converted it into a young, fertile lithospheric mantle through melt-rock reaction.

Basalt-hosted mantle xenoliths in the < 108 Ma mafic rocks provide valuable clues for such processes. Xenoliths in the Fuxin basalts are composed of lherzolite xenoliths with olivine Mg# ~90, high-Mg harzburgite xenoliths (olivine Mg# > 92), and minor lherzolite xenoliths with olivine Mg# ~86 (Zheng et al., 2007). The first type of lherzolite xenoliths contains clinopyroxene with high Nb concentrations, precluding H_2O-rich fluids as the metasomatic agent. Meanwhile, these clinopyroxene crystals have high Ti/Eu and low La/Yb, indicating of silicate-melt metasomatism (Zheng et al., 2007). Mantle xenoliths in the Late Cretaceous mafic rocks in Shandong Peninsula are also dominantly fertile lherzolite (olivine Mg# < 90) with minor refractory high-Mg peridotite xenoliths (Ying et al., 2006; Zheng, 2009; Zheng

et al., 2007). The high-Mg lherzolite xenoliths contain clinopyroxene with enriched LREE, high $^{87}Sr/^{86}Sr$ (0.704116–0.708695) and low $^{143}Nd/^{144}Nd$ (0.512152–0.512921), while clinopyroxene in low-Mg lherzolite xenoliths shows low total REE contents and depleted Sr-Nd isotopic compositions (Zhang, 2009). Such low-Mg lherzolite is generally considered as newly accreted lithospheric mantle that replaced the old and refractory lithospheric mantle through melt-peridotite interaction, while high-Mg peridotite represents relicts of ancient lithospheric mantle (Xu, 2001; Zhang et al., 2005, 2011; Zheng et al., 2007, 1998). In other words, with continuous melt injections and melt-rock interactions, the ancient lithospheric mantle with enriched geochemical and isotopic compositions was gradually transformed into a newly accreted lithospheric mantle with depleted isotopic compositions and low LILE (LREE) contents. That's why the enriched components observed in the Early Cretaceous basalts were essentially absent in the Tertiary basalts (Lu et al., 2006; Xu, 2014). Finally, both Cenozoic basalts and xenoliths are mainly characterized by depleted Sr-Nd isotopic compositions (OIB-like) (Fan et al., 2000).

5. Conclusion

Major geochemical and isotopic transition in continental basalts occurred at ~108 Ma in the NCC, when primary sources of basalts changed from the metasomatized lithospheric mantle to asthenosphere. Metasomatism was pervasive in lithospheric mantle beneath the NCC in the Early Cretaceous. Decreasing extent of metasomatism from the east to the west beneath the NCC indicates that the westward subduction of the Paleo-Pacific plate was likely responsible to Cretaceous basaltic activities in the NCC. The < 108 Ma Cretaceous basalts have “OIB-like” geochemical characteristics, but slightly enriched fluid mobile elements (e.g. Ba, Pb and Sr) relative to typical OIB. The primary source of the < 108 Ma Cretaceous alkali basalts is asthenosphere, but asthenosphere-derived melts may be “contaminated” by varying proportion of subduction enriching components in relict metasomatized lithospheric mantle. Flat subduction of the spreading ridge between the Izanagi and Pacific plates was intimately bound up with the Cretaceous magmatism and geodynamic evolution of the NCC. The destruction of the NCC may result from a joint effect of hydration, subduction erosion and thermal-chemical erosion, but the first-order dynamic trigger may be flat subduction of the ridge between the Pacific and Izanagi plates, and subsequent slab rollback.

Acknowledgements

We would like to thank Prof. Klaus Mezger and two anonymous reviewers for the handling and constructive review comments on our manuscript. This study was supported by National Key R & D Program of China (2016YFC0600408), Natural Science Foundation of China (91328204 and 41421062), Guangdong Natural Science Funds (2014A030306032 and 2015TQ01Z611) and Youth Innovation Promotion Association CAS (2016315). This is contribution No. IS-2429 from GIG-CAS.

Appendix A. Supplementary data

Supplementary data to this article can be found online at http://dx.doi.org/10.1016/j.chemgeo.2017.08.025.

References

Albarède, F., 2003. Geochemistry: An Introduction. Cambridge University Press, pp. 223–229.
Anderson, A.T., 1982. Parental basalts in subduction zones: implications for continental evolution. J. Geophys. Res. 87, 7047–7060.
Antonijevic, S.K., et al., 2015. The role of ridges in the formation and longevity of flat slabs. Nature 524, 212–215.
Asimow, P.D., Langmuir, C., 2003. The importance of water to oceanic mantle melting regimes. Nature 421, 815–820.
Beard, B.L., Johnson, C.M., 1997. Hafnium isotope evidence for the origin of Cenozoic basaltic lavas from the southwestern United States. J. Geophys. Res. 102, 20149–20178.
Bebout, G., 2014. Chemical and isotopic cycling in subduction zones. In: Treatise on Geochemistry, Second edition. 4. pp. 703–747.
Bonadiman, C., Hao, Y.T., Coltorti, M., Dallai, L., Faccini, B., Huang, Y., Xia, Q.K., 2009. Water contents of pyroxenes in intraplate lithospheric mantle. Eur. J. Mineral. 21, 637–647.
Burke, K., Steinberger, B., Torsvik, T.H., Smethurst, M.A., 2008. Plume generation zones at margins of large low shear velocity provinces on the core-mantle boundary. Earth Planet. Sci. Lett. 265, 49–60.
Cameron, B.I., Walker, J.A., Carr, M.J., Patino, L.C., Matìas, O., Feigenson, M.D., 2003. Flux versus decompression melting at stratovolcanoes in southeastern Guatemala. J. Volcanol. Geotherm. Res. 119 (1-4), 21–50.
Chen, Y., Zhu, G., Jiang, D.Z., Lin, S.Z., 2014. Deformation characteristics and formation mechanism of the Yunmengshan metamorphic core complex. Chin. Sci. Bull. 59, 1525–1541.
Clift, P.D., Vannucchi, P., Morgan, J.P., 2009. Crustal redistribution, crust–mantle recycling and Phanerozoic evolution of the continental crust. Earth Sci. Rev. 97, 80–104.
Crow, R., Karlstrom, K., Asmerom, Y., Schmandt, B., Polyak, V., Dufrane, S.A., 2010. Shrinking of the Colorado Plateau via lithospheric mantle erosion: evidence from Nd and Sr isotopes and geochronology of Neogene basalts. Geology 39, 27–30.
Dai, L.Q., Zheng, Y.F., Zhao, Z.F., 2016. Termination time of peak decratonization in North China: geochemical evidence from mafic igneous rocks. Lithos s240–243, 327–336.
Davis, G.A., Zheng, Y., Wang, C., Darby, B.J., Zhang, Ch., Gehrels, G.E., 2001. Mesozoic tectonic evolution of the Yanshan fold and thrust belt, with emphasis on Hebei and Liaoning provinces, northern China. Mem. Geol. Soc. Am. 194, 171–194.
DePaolo, D.J., Daley, E.E., 2000. Neodymium isotopes in basalts of the southwest basin and range and lithospheric thinning during continental extension. Chem. Geol. 169, 157–185.
Elliott, T., Plank, T., Zindler, A., White, W., Bourdon, B., 1997. Element transport from slab to volcanic front at the Mariana arc. J. Geophys. Res. 102, 14991–15019.
Falloon, T., Green, D., Hatton, C., Harris, K., 1988. Anhydrous partial melting of a fertile and depleted peridotite from 2 to 30 kb and application to basalt petrogenesis. J. Petrol. 29, 1257–1282.
Fan, W.M., Menzies, M., 1992. Destruction of aged lower lithosphere and accretion of asthenosphere mantle beneath eastern China. Geotecton. Metallog. 16, 171–180.
Fan, W.M., Zhang, H.F., Baker, J., Jarvis, K.E., Mason, P.R.D., Menzies, M.A., 2000. On and off the North China Craton: where is the Archaean keel? J. Petrol. 41, 933–950.
Farmer, G.L., 2014. Continental basaltic rocks. In: Treatise on Geochemistry, Second edition. 4. pp. 75–110.
Farmer, G.L., Glazner, A.F., Wilshire, H.G., Wooden, J.L., et al., 1995. Origin of Late Cenozoic basalts at the Cima volcanic field, Mojave Desert, California. J. Geophys. Res. 100, 8399–8415.
Fitton, J.G., 2007. The OIB paradox. In: Foulger, G.R., Jurdy, D.M. (Eds.), Plates, Plumes, and Planetary Processes. Geol. Soc. America Special Paper 430. pp. 387–412.
Fitton, J., James, D., Kempton, P., Ormerod, D., Leeman, W., 1988. The role of lithospheric mantle in the generation of late Cenozoic basic magmas in the western United States. J. Petrol. (1), 331–349.
Fitton, J.G., James, D., Leeman, W.P., 1991. Basic magmatism associated with late Cenozoic extension in the western United States: compositional variations in space and time. J. Geophys. Res. 96, 13693–13711.
Gaetani, G.A., Grove, T.L., 1998. The influence of water on melting of mantle peridotite. Contrib. Mineral. Petrol. 131, 323–346.
Gao, S., Rudnick, R.L., Carlson, R.W., McDonough, W.F., Liu, Y.S., 2002. Re–Os evidence for replacement of ancient mantle lithosphere beneath the North China craton. Earth Planet. Sci. Lett. 198, 307–322.
Gao, S., Rudnick, R.L., Yuan, H.L., Liu, X.M., Liu, Y.S., Xu, W.L., Ling, W.L., Ayers, J., Wang, X.C., Wang, Q.H., 2004. Recycling lower continental crust in the North China craton. Nature 432, 892–897.
Gao, S., Rudnick, R.L., Xu, W.L., Yuan, H.L., Liu, Y.S., Walker, R.J., Puchtel, I.S., Liu, X., Huang, H., Wang, X.R., Yang, J., et al., 2008. Recycling deep cratonic lithosphere and generation of intraplate magmatism in the North China Craton. Earth Planet. Sci. Lett. 270, 41–53.
Griffin, W.L., Andi, Z., O'reilly, S.Y., Ryan, C.G., 1998. Phanerozoic evolution of the lithosphere beneath the Sino-Korean craton. In: Flower, M.F.J., Chung, S.-L., Lo, C.-H., Lee, T.-Y. (Eds.), Mantle Dynamics and Plate Interactions in East Asia. Geodyn. Ser, vol. 27. Am. Geophy. Union, Washington, DC, pp. 107–126.
Guo, J.T., Guo, F., Wang, C.Y., Li, C.W., 2013. Crustal recycling processes in generating the early Cretaceous Fangcheng basalts, North China Craton: new constraints from mineral chemistry, oxygen isotopes of olivine and whole-rock geochemistry. Lithos 170, 1–16.
Guo, P.Y., et al., 2014. Lithosphere thinning beneath west North China Craton: evidence from geochemical and Sr–Nd–Hf isotope compositions of Jining basalts. Lithos 202, 37–54.
Hart, S.R., Hauri, E.H., Oschmann, L.A., Whitehead, J.A., 1992. Mantle plumes and entrainment: isotopic evidence. Science 256, 517–520.
Hawkesworth, C., Rogers, N., Van Calsteren, P., Menzies, M., 1984. Mantle enrichment processes. Nature 311, 331–335.
Hofmann, A., 1997. Mantle geochemistry: the message from oceanic volcanism. Nature 385, 219–229.
Hofmann, A., 2003. Sampling mantle heterogeneity through oceanic basalts: isotopes and trace elements. In: Treatise on Geochemistry. 2. pp. 61–101.

Hole, M.J., Rogers, G., Saunders, A.D., Storey, M., 1991. Relation between alkalic volcanism and slab-window formation. Geology 19, 657–660.
Huang, J.L., Zhao, D.P., 2006. High-resolution mantle tomography of China and surrounding regions. J. Geophys. Res. 111, B09305.
Jahn, B.M., Wu, F.Y., Lo, C.H., Tsai, C.H., 1999. Crust–mantle interaction induced by deep subduction of the continental crust: geochemical and Sr–Nd isotopic evidence from post-collisional mafic–ultramafic intrusions of the northern Dabie complex, central China. Chem. Geol. 157, 119–146.
Johnson, E.R., Wallace, P.J., Granados, H.D., Manea, V.C., Kent, A.J.R., Bindeman, I.N., Donegan, C.S., 2009. Subduction-related volatile recycling and magma generation beneath Central Mexico: insights from melt inclusions, oxygen isotopes and geodynamic models. J. Petrol. 50, 1729–1764.
Jordán, T.E., Isacks, B.L., Allmendinger, R.W., Brewer, J.A., Ramos, V.A., Ando, C.J., 1983. Andean tectonics related to geometry of subducted Nazca plate. Geol. Soc. Am. Bull. 94, 341–361.
Kelemen, P., Hanghøj, K., Greene, A., 2003. One view of the geochemistry of subduction-related magmatic arcs, with an emphasis on primitive andesite and lower crust. In: Treatise on Geochemistry. 3. pp. 593–659.
Kempton, P.D., Fitton, J.G., Hawkesworth, C.J., Ormerod, D.S., 2011. Isotopic and trace element constraints on the composition and evolution of the lithosphere beneath the southwestern United States. J. Geophys. Res. 9, 13713–13735.
Keppler, H., 1996. Constraints from partitioning experiments on the composition of subduction-zone fluids. Nature 380, 237–240.
Kinoshita, O., 1995. Migration of igneous activities related to ridge subduction in Southwest Japan and the east-Asian continental-margin from the Mesozoic to the Paleogene. Tectonophysics 245, 25–35.
Kusky, T.M., Windley, B.F., Zhai, M.G., 2007. Lithospheric thinning in eastern Asia; constraints, evolution, and tests of models. Geol. Soc. Lond. Spec. Publ. 280, 331–343.
Li, Z.X., Li, X.H., 2007. Formation of the 1300-km-wide intracontinental orogen and postorogenic magmatic province in Mesozoic South China: a flat-slab subduction model. Geology 35, 179–182.
Li, J., Yuen, D.A., 2014. Mid-mantle heterogeneities associated with Izanagi plate: implications for regional mantle viscosity. Earth Planet. Sci. Lett. 385, 137–144.
Li, H., Zhang, H., Ling, M.X., Wang, F.Y., Ding, X., Zhou, J.B., Yang, X.Y., Tu, X.L., Sun, W.D., 2011. Geochemical and zircon U-Pb study of the Huangmeijian A-type granite: implications for geological evolution of the Lower Yangtze River belt. Int. Geol. Rev. 53, 499–525.
Li, H., Ling, M.X., Li, C.Y., Zhang, H., Ding, X., Yang, X.Y., Fan, W.M., Li, Y.L., Sun, W.D., 2012a. A-type granite belts of two chemical subgroups in central eastern China: indication of ridge subduction. Lithos 150, 26–36.
Li, S.Z., Zhao, G.C., Dai, L.M., Liu, X., Zhou, L.H., Santosh, M., Suo, Y.H., 2012b. Mesozoic basins in eastern China and their bearing on the deconstruction of the North China Craton. J. Asian Earth Sci. 47, 64–79.
Li, J., Wang, X., Wang, X.J., Yuen, D.A., 2013. P and SH velocity structure in the upper mantle beneath Northeast China: evidence for a stagnant slab in hydrous mantle transition zone. Earth Planet. Sci. Lett. 367, 71–81.
Li, H., Ling, M.X., Ding, X., Zhang, H., Li, C.Y., Liu, D.Y., Sun, W.D., 2014. The geochemical characteristics of Haiyang A-type granite complex in Shandong, eastern China. Lithos 200, 142–156.
Li, P., Xia, Q.K., Deloule, E., Chen, H., Gu, X.Y., Feng, M., 2015. Temporal variation of H_2O content in the lithospheric mantle beneath the eastern North China Craton: implications for the destruction of cratons. Gondwana Res. 28, 276–287.
Lin, W., Faure, M., Chen, Y., Ji, W.B., Wang, F., Wu, L., Charles, N., Wang, J., Wang, Q.C., 2013a. Late Mesozoic compressional to extensional tectonics in the Yiwulüshan massif, NE China and its bearing on the evolution of the Yinshan-Yanshan orogenic belt Part I: structucral analyses and geochronological constraints. Gondwana Res. 23, 54–77.
Lin, W., Charles, N., Chen, Y., Chen, K., Faure, M., Wu, L., Wang, F., Li, Q.L., Wang, J., Wang, Q.C., 2013b. Late Mesozoic compressional to extensional tectonics in the Yiwulüshan massif, NE China and its bearing on the evolution of the Yinshan-Yanshan orogenic belt Part II: anisotropy of magnetic susceptibility and gravity modeling. Gondwana Res. 23, 78–94.
Ling, M.X., et al., 2009. Cretaceous ridge subduction along the lower Yangtze River belt, eastern China. Econ. Geol. 104, 303–321.
Ling, M.X., et al., 2013. Destruction of the North China Craton induced by ridge subductions. J. Geol. 121, 197–213.
Liu, Y.S., Gao, S., Kelemen, P.B., Xu, W.L., 2008. Recycled crust controls contrasting source compositions of Mesozoic and Cenozoic basalts in the North China Craton. Geochim. Cosmochim. Acta 72, 2349–2376.
Liu, S.A., Li, S.G., He, Y.S., Huang, F., 2010. Geochemical contrasts between early Cretaceous ore-bearing and ore-barren high-Mg adakites in central-eastern China: implications for petrogenesis and Cu-Au mineralization. Geochim. Cosmochim. Acta 74 (24), 7160–7178.
Lu, F.X., et al., 2006. Asthenospheric upwelling and lithospheric thinning in late Cretaceous-Cenozoic in eastern North China. Earth Sci. Front. 13, 86–92 (in Chinese with English abstract).
Ma, L., et al., 2014. Lithospheric and asthenospheric sources of lamprophyres in the Jiaodong Peninsula: a consequence of rapid lithospheric thinning beneath the North China Craton? Geochim. Cosmochim. Acta 124, 250–271.
Ma, L., et al., 2016. Rapid lithospheric thinning of the North China Craton: new evidence from cretaceous mafic dikes in the Jiaodong Peninsula. Chem. Geol. 432, 1–15.
Maruyama, S., Isozaki, Y., Kimura, G., Terabayashi, M., 1997. Paleogeographic maps of the Japanese Islands: plate tectonic synthesis from 750 Ma to the present. Island Arc 6, 121–142.
McCulloch, M.T., Gamble, J., 1991. Geochemical and geodynamical constraints on subduction zone magmatism. Earth Planet. Sci. Lett. 102, 358–374.
McDonough, W.F., 1991. Partial melting of subducted oceanic crust and isolation of its residual eclogitic lithology. Philos. Trans. R. Soc. Lond. A 335, 407–418.
Mckenzie, D., Bickle, M.J., 1988. The volume and composition of melt generated by extension of the lithosphere. J. Petrol. 29, 625–679.
Meng, F.X., Gao, S., Niu, Y.L., Liu, Y.S., Wang, X.R., 2015. Mesozoic–Cenozoic mantle evolution beneath the North China Craton: a new perspective from Hf–Nd isotopes of basalts. Gondwana Res. 27, 1574–1585.
Menzies, M.A., Xu, Y.G., Zhang, H.F., Fan, W.M., 2007. Integration of geology, geophysics and geochemistry: a key to understanding the North China Craton. Lithos 96 (1–2), 1–21.
Ni, S.D., Tan, E., Gurnis, M., Helmberger, D., 2002. Sharp sides to the African superplume. Science 296, 1850–1852.
Niu, Y.L., 2005. Generation and evolution of basaltic magmas: some basic concepts and a new view on the origin of Mesozoic–Cenozoic basaltic volcanism in eastern China. Geol. J. China Univ. 11, 9–46.
Niu, Y.L., O'Hara, M.J., 2003. Origin of ocean island basalts: a new perspective from petrology, geochemistry, and mineral physics considerations. J. Geophys. Res. 108, B42209.
Niu, Y., et al., 2015. Exotic origin of the Chinese continental shelf: new insights into the tectonic evolution of the western Pacific and eastern China since the Mesozoic. Chin. Sci. Bull. 60, 1598–1616.
Ormerod, D.S., Hawkesworth, C.J., Rogers, N.W., Leeman, W.P., Menzies, M.A., 1988. Tectonic and magmatic transitions in the western Great-Basin, USA. Nature 333, 349–353.
Pang, C.J., Wang, X.C., Xu, Y.G., Wen, S.N., Kuang, Y.S., Hong, L.B., 2015. Pyroxenite-derived Early Cretaceous lavas in the Liaodong Peninsula: implication for metasomatism and thinning of the lithospheric mantle beneath North China Craton. Lithos 227, 77–93.
Plank, T., Langmuir, C.H., 1998. The chemical composition of subducting sediments and its consequences for the crust and mantle. Chem. Geol. 145, 325–394.
Presnall, D.C., Dixon, S.A., Dixon, J.R., O'Donnell, T.H., Brenner, N.L., Schrock, R.L., Dycus, D.W., 1978. Liquidus phase relations on the join diopside-forsterite-anorthite from 1 atm to 20 kbar: their bearing on the generation and crystallization of basaltic magma. Contrib. Mineral. Petrol. 66, 203–220.
Ramos, V.A., Cristallini, E., Pérez, D.J., 2002. The Pampean flat-slab of the Central Andes. J. S. Am. Earth Sci. 15, 59–78.
Reiners, P.W., Hammond, P.E., McKenna, J.M., Duncan, R.A., 2000. Young basalts of the central Washington Cascades, flux melting of the mantle, and trace element signatures of primary arc magmas. Contrib. Mineral. Petrol. 138, 249–264.
Ren, J., Tamaki, K., Li, S., Zhang, J.X., 2002. Late Mesozoic and Cenozoic rifting and its dynamic setting in eastern China and adjacent areas. Tectonophysics 344, 175–205.
Rudnick, R.L., Gao, S., 2003. Composition of the continental crust. In: Treatise on Geochemistry. 3. pp. 1–64.
Ryan, J.G., Chauvel, C., 2014. The subduction-zone filter and the impact of recycled materials on the evolution of the mantle. In: Treatise on Geochemistry. 3. pp. 479–508.
Sagong, H., Kwon, S., Ree, J., 2005. Mesozoic episodic magmatism in South Korea and its tectonic implication. Tectonics 24, 125–127.
Sakaguchi, A., 1996. High paleogeothermal gradient with ridge subduction beneath the Cretaceous Shimanto accretionary prism, southwest Japan. Geology 24, 795–798.
Saunders, A.D., Storey, M., Kent, R., Norry, M., 1992. Consequences of plume-lithosphere interactions. Geol. Soc. Spec. Publ. 68, 41–60.
Sengör, A.M.C., Natal'in, B.A., 1996. Paleotectonics of Asia: fragments of a synthesis. In: Yin, A., Harrisn, T.M. (Eds.), The Tectonic Evolution of Asia. Cambridge University Press, Cambridge, pp. 486–641.
Seton, M., Müller, R.D., Zahirovic, S., Gaina, C., Torsvik, T., Shephard, G., Talsma, A., Gurnis, M., Turner, M., Maus, S., Chandler, M., 2012. Global continental and ocean basin reconstructions since 200 Ma. Earth-Sci. Rev. 113, 212–270.
Stolper, E., Newman, S., 1994. The role of water in the petrogenesis of Mariana trough magmas. Earth Planet. Sci. Lett. 121, 293–325.
Straub, S., Goldstein, S., Class, C., Schmidt, A., 2009. Mid-ocean-ridge basalt of Indian type in the northwest Pacific Ocean basin. Nat. Geosci. 2, 286–289.
Sun, W.D., 2015. Decratonic gold deposits: a new concept and new opportunities. Natl. Sci. Rev. 2, 248–252.
Sun, S.S., McDonough, W., 1989. Chemical and isotopic systematics of oceanic basalts: implications for mantle composition and processes. Geol. Soc. Spec. Publ. 42, 313–345.
Sun, W.D., Bennett, V.C., Kamenetsky, V.S., 2004. The mechanism of Re enrichment in arc magmas: evidence from Lau Basin basaltic glasses and primitive melt inclusions. Earth Planet. Sci. Lett. 222, 101–114.
Sun, W.D., Ding, X., Hu, Y.H., Li, X.H., 2007. The golden transformation of the Cretaceous plate subduction in the west Pacific. Earth Planet. Sci. Lett. 262, 533–542.
Sun, W.D., Hu, Y.H., Kamenetsky, V.S., Eggins, S.M., Chen, M., Arculus, R.J., 2008. Constancy of Nb/U in the mantle revisited. Geochim. Cosmochim. Acta 72, 3542–3549.
Sun, W.D., Ling, M.X., Yang, X.Y., Fan, W.M., Ding, X., Liang, H.Y., 2010. Ridge subduction and porphyry copper-gold mineralization: an overview. Sci. China Earth Sci. 53, 475–484.
Sun, W.D., Li, S., Yang, X.Y., Ling, M.X., Ding, X., Duan, L.A., Zhan, M.Z., Zhang, H., Fan, W.M., 2013. Large-scale gold mineralization in eastern China induced by an Early Cretaceous clockwise change in Pacific plate motions. Int. Geol. Rev. 55, 311–321.
Turner, S., Hawkesworth, C., 1997. Constraints on flux rates and mantle dynamics beneath island arcs from Tonga-Kermadec lava geochemistry. Nature 389, 568–573.
Turner, S.J., Langmuir, C.H., 2015. The global chemical systematics of arc front stratovolcanoes: evaluating the role of crustal processes. Earth Planet. Sci. Lett. 422,

182–193.
Walker, J.A., Roggensack, K., Patino, L.C., Cameron, B.I., Matías, O., 2003. The water and trace element contents of melt inclusions across an active subduction zone. Contrib. Mineral. Petrol. 146, 62–77.
Wang, Q., Wyman, D.A., Xu, J.F., Zhao, Z.H., Jian, P., Xiong, X.L., Bao, Z.W., Li, C.F., Bai, Z.H., 2006. Petrogenesis of Cretaceous adakitic and shoshonitic igneous rocks in the Luzong area, Anhui Province (eastern China): implications for geodynamics and Cu–Au mineralization. Lithos 89, 424–446.
Wang, Q., Wyman, D.A., Xu, J.F., Zhao, Z.H., Jian, P., Zi, F., 2007. Partial melting of thickened or delaminated lower crust in the middle of eastern China: implications for Cu–Au mineralization. J. Geol. 115, 149–161.
Wang, Z.S., Kusky, T.M., Capitanio, F.A., 2016. Lithosphere thinning induced by slab penetration into a hydrous mantle transition zone. Geophys. Res. Lett. 43, 11567–11577.
Weaver, B.L., 1991. The origin of ocean island basalt end-member compositions - trace-element and isotopic constraints. Earth Planet. Sci. Lett. 104, 381–397.
Windley, B.F., Maruyama, S., Xiao, W.J., 2010. Delamination/thinning of sub-continental lithospheric mantle under eastern China: the role of water and multiple subduction. Am. J. Sci. 310, 1250–1293.
Wu, F.Y., Sun, D.Y., Li, H.M., Jahn, B.M., Wilde, S., 2002. A-type granites in northeastern China: age and geochemical constraints on their petrogenesis. Chem. Geol. 187, 143–173.
Wu, F.Y., Lin, J.Q., Wilde, S.A., Zhang, X.O., Yang, J.H., 2005. Nature and significance of the Early Cretaceous giant igneous event in eastern China. Earth Planet. Sci. Lett. 233, 103–119.
Wu, F.Y., Walker, R.J., Yang, Y.H., Yuan, H.L., Yang, J.H., 2006. The chemical-temporal evolution of lithospheric mantle underlying the North China Craton. Geochim. Cosmochim. Acta 70, 5013–5034.
Xia, Q.K., et al., Hao, Y.T., Li, P., Delouble, E., Coltorti, M., Dallai, L., Yang, X.Z., Feng, M., 2010. Low water content of the Cenozoic lithospheric mantle beneath the eastern part of the North China Craton. J. Geophys. Res. 115, B07207.
Xia, Q.K., Hao, Y.T., Liu, S.C., Gu, X.Y., Feng, M., 2013a. Water contents of the Cenozoic lithospheric mantle beneath the western part of the North China Craton: peridotite xenolith constraints. Gondwana Res. 23, 108–118.
Xia, Q.K., et al., Liu, J., Liu, S.C., Kovács, I., Feng, M., Dang, L., 2013b. High water content in Mesozoic primitive basalts of the North China Craton and implications on the destruction of cratonic mantle lithosphere. Earth Planet. Sci. Lett. 361, 85–97.
Xu, Y.G., 2001. Thermo-tectonic destruction of the Archaean lithospheric keel beneath the Sino-Korean Craton in China: evidence, timing and mechanism. Phys. Chem. Earth A 26, 747–757.
Xu, Y.G., 2014. Recycled oceanic crust in the source of 90–40 Ma basalts in North and Northeast China: evidence, provenance and significance. Geochim. Cosmochim. Acta 143, 49–67.
Xu, Y.G., Huang, X.L., Ma, J.L., Wang, Y.B., Iizuka, Y., Xu, J.F., Wang, Q., Wu, X.Y., 2004. Crust-mantle interaction during the tectono-thermal reactivation of the North China Craton: constraints from SHRIMP zircon U–Pb chronology and geochemistry of Mesozoic plutons from western Shandong. Contrib. Mineral. Petrol. 147, 750–767.
Xu, Y.G., Li, H.Y., Pang, C.J., He, B., 2009. On the timing and duration of the destruction of the North China Craton. Chin. Sci. Bull. 54, 3379–3396.
Yang, W., Li, S.G., 2008. Geochronology and geochemistry of the Mesozoic volcanic rocks in western Liaoning: implications for lithospheric thinning of the North China Craton. Lithos 102, 88–117.
Yang, X.Z., Xia, Q.K., Deloule, E., Dallai, L., Fan, Q.C., Feng, M., 2008. Water in minerals of the continental lithospheric mantle and overlying lower crust: a comparative study of peridotite and granulite xenoliths from the North China Craton. Chem. Geol. 256, 33–45.
Yang, Y.H., Wu, F.Y., Wilde, S.A., Liu, X.M., Zhang, Y.B., Xie, L.W., Yang, J.H., 2009. In situ perovskite Sr–Nd isotopic constraints on the petrogenesis of the Ordovician Mengyin kimberlites in the North China Craton. Chem. Geol. 264, 24–42.
Yang, W., Teng, F.Z., Zhang, H.F., Li, S.G., 2012. Magnesium isotopic systematics of continental basalts from the North China craton: implications for tracing subducted carbonate in the mantle. Chem. Geol. 328, 185–194.
Ying, J.F., Zhang, H.F., Kita, N., Morishita, Y.C., Shimoda, G., 2006. Nature and evolution of Late Cretaceous lithospheric mantle beneath the eastern North China Craton: constraints from petrology and geochemistry of peridotitic xenoliths from Jünan, Shandong Province, China. Earth Planet. Sci. Lett. 244, 622–638.
Zhang, H.F., 2005. Transformation of lithospheric mantle through peridotite-melt reaction: a case of Sino-Korean craton. Earth Planet. Sci. Lett. 237, 768–780.
Zhang, H.F., 2009. Peridotite-melt interaction: a key point for the destruction of cratonic lithospheric mantle. Chin. Sci. Bull. 54, 3417–3437.
Zhang, H.F., Yang, Y., 2007. Emplacement age and Sr-Nd-Hf isotopic characteristics of the diamondiferous kimberlites from the eastern North China Craton. Acta Petrol. Sin. 23, 285–294 (In Chinese with English abstract).
Zhang, H.F., Zheng, J.P., 2003. Geochemical characteristics and petrogenesis of Mesozoic basalts from the North China Craton: a case study in Fuxin, Liaoning Province. Chin. Sci. Bull. 48, 924–930.
Zhang, H.F., Sun, M., Zhou, X.H., Fan, W.M., Zhai, M.G., Yin, J.F., 2002. Mesozoic lithosphere destruction beneath the North China Craton: evidence from major-, trace-element and Sr-Nd-Pb isotope studies of Fangcheng basalts. Contrib. Mineral. Petrol. 144, 241–254.
Zhang, H.F., Sun, M., Zhou, X.H., Zhou, M.F., Fan, W.M., Zheng, J.P., 2003a. Secular evolution of the lithosphere beneath the eastern North China Craton: evidence from Mesozoic basalts and high-Mg andesites. Geochim. Cosmochim. Acta 67, 4373–4387.
Zhang, Y.Q., Dong, S.W., Shi, W., 2003b. Cretaceous deformation history of the middle Tan-Lu fault zone in Shandong Province, eastern China. Tectonophysics 363, 243–258.
Zhang, H.F., Zhou, X.H., Fan, W.M., Sun, M., Guo, F., Ying, J.F., Tang, Y.J., Zhang, J., Niu, L.F., 2005. Nature, composition, enrichment processes and its mechanism of the Mesozoic lithospheric mantle beneath the southeastern North China Craton. Acta Petrol. Sin. 21, 1271–1280.
Zhang, H.F., Goldstein, S.L., Zhou, X.H., Sun, M., Zheng, J.P., Cai, Y., 2008a. Evolution of subcontinental lithospheric mantle beneath eastern China: Re–Os isotopic evidence from mantle xenoliths in Paleozoic kimberlites and Mesozoic basalts. Contrib. Mineral. Petrol. 155, 271–293.
Zhang, Y.Q., Li, J.L., Zhang, T., Dong, S.W., Yuan, J.Y., 2008b. Cretaceous to Paleocene tectono-sedementary evolution of the Jiaolai basin and the contineous areas of the Shandong peninsula (North China) and its geodynamic implications. Acta Geol. Sin. 82, 1229–1257.
Zhang, J.J., Zheng, Y.F., Zhao, Z.F., 2009. Geochemical evidence for interaction between oceanic crust and lithospheric mantle in the origin of Cenozoic continental basalts in east-central China. Lithos 110, 305–326.
Zhang, J., Zhang, H.F., Kita, N., Shimoda, G., Morishita, Y., Ying, J.F., Tang, Y.J., 2011. Secular evolution of the lithospheric mantle beneath the eastern North China craton: evidence from peridotitic xenoliths from Late Cretaceous mafic rocks in the Jiaodong region, east-central China. Int. Geol. Rev. 53, 182–211.
Zhang, H., Li, C.Y., Yang, X.Y., Sun, Y.L., Deng, J.H., Liang, H.Y., Wang, R.L., Wang, B.H., Wang, Y.X., Sun, W.D., 2014. Shapinggou: the largest climax-type porphyry Mo deposit in China. Int. Geol. Rev. 56, 313–331.
Zhao, G.C., Wilde, S.A., Cawood, P.A., Sun, M., 2001. Archean blocks and their boundaries in the North China Craton: lithological, geochemical, structural and P–T path constraints and tectonic evolution. Precambrian Res. 107, 45–73.
Zhao, Y., Xu, G., Zhang, S., Yang, Z., Zhang, Y., Hu, J., 2004. Yanshanian movement and conversion of tectonic regimes in eastern Asia. Earth Sci. Front. 11, 319–328.
Zheng, J.P., 1999. Mesozoic–Cenozoic Mantle Replacement and Lithospheric Thinning. 126 China University of Geosciences Press, Wuhan.
Zheng, J.P., 2009. Comparison of mantle-derived materials from different spatiotemporal settings: implications for destructive and accretional processes of the North China Craton. Chin. Sci. Bull. 54, 3397–3416.
Zheng, J.P., Lu, F.X., 1999. Petrologic characteristics of kimberliteborne mantle xenoliths from the Shandong and Liaoning Peninsula: paleozoic lithosphere mantle and its heterogeneity (in Chinese with English abstract). Acta Petrol. Sin. 15, 65–74.
Zheng, Y.F., Wu, F.Y., 2009. Growth and reworking of cratonic lithosphere. Chin. Sci. Bull. 54, 3347–3353.
Zheng, J.P., O'reilly, S.Y., Griffin, W.L., Lu, F.X., Zhang, M., 1998. Nature and evolution of Cenozoic lithospheric mantle beneath Shandong peninsula, Sino-Korean craton, eastern China. Int. Geol. Rev. 40, 471–499.
Zheng, J.P., Griffin, W.L., O'Reilly, S.Y., Yu, C.M., Zhang, H.F., Pearson, N., Zhang, M., 2007. Mechanism and timing of lithospheric modification and replacement beneath the eastern North China Craton: peridotitic xenoliths from the 100 Ma Fuxin basalts and a regional synthesis. Geochim. Cosmochim. Acta 71, 5203–5225.
Zhu, R.X., Zheng, T.Y., 2009. Destruction geodynamics of the North China craton and its Paleoproterozoic plate tectonics. Chin. Sci. Bull. 54, 3354–3366.
Zhu, R.X., Chen, L., Wu, F.Y., Liu, J.L., 2011. Timing, scale and mechanism of the destruction of the North China Craton. Sci. China Earth Sci. 54, 789–797.
Zhu, R.X., Xu, Y.G., Zhu, G., Zhang, H.F., Xia, Q.K., Zheng, T.Y., 2012a. Destruction of the North China Craton. Sci. China Earth Sci. 55, 1565–1587.
Zhu, R.X., Yang, J.H., Wu, F.Y., 2012b. Timing of destruction of the North China Craton. Lithos 149, 51–60.
Zhu, R.X., Fan, H.R., Li, J.W., Meng, Q.R., Li, S.R., Zeng, Q.D., 2015. Decratonic gold deposits. Sci. China Earth Sci. 58, 1523–1537.